**Numerical Modelling of Tectonic Evolutuin of the Wadati-Benioff Zone Beneath the Andean Region. The Extended version**

Berrocal, J.
2001

**Institute of Computer Science**
**Academy of Sciences of the Czech Republic**

# Numerical Modelling of Tectonic Evolution of the Wadati-Benioff Zone Beneath the Andean Region (The Extended Version)

Jesus Berrocal, Jiří Nedoma, Zdeněk Kestřánek

Technical report No. 842

2001

Pod Vodárenskou věží 2, 182 07 Prague 8, phone: (+4202) 6605 1111, fax: (+4202) 858 57 89,
e-mail:nedoma@cs.cas.cz

# NUMERICAL MODELLING OF TECTONIC EVOLUTION OF THE WADATI-BENIOFF ZONE BENEATH THE ANDEAN REGION. THE EXTENDED VERSION.

JESUS BERROCAL†, JIŘÍ NEDOMA‡, AND ZDENĚK KESTŘÁNEK‡

*Technical Report No V-842, ICS AS CR, Prague, 2001*

ABSTRACT. Important controversies exist about the seismotectonic characterisrics in the Andean region, in relation both to the morphology of the Wadati-Benioff zone (WBZ) and to the focal mechanism responsible for the very deep (h>500km) South American earthquakes.

Based on numerical modelling and the use of good quality relocated hypocentres, and other tectonic data, we propose to demonstrate that the Nazca slab portion among 24°S and 01◦S, is in a process of a top-to the north shear in such a way that its deep corresponding extremes seem to be, at present times, at latitudes 29°S and 06°S, respectively. The seismic data also permitted to elaborate an updatad and more detailed contour map of the WBZ topography. In this map it is possible to correlate the change on the slab's dip beneath the central and northern Peruvian regions with the subduction of the Nazca aseismic ridge and with a probable north-western migration of the slab comprising the subducted oceanic ridge. The hypothesis presented in this paper, that suggests a northwards translation of the slab in the transition zone at around 600km depth, permits to infer a flat horizontal mechanism for the very deep South American earthquakes, similarly to the focal mechanism determined for the large deep Bolivian event of June 1994.

Numerical modelling of this framework is based on the plate tectonic hypothesis and the theory of contact problems with friction in (thermo-)elasticity. We shall assume that the Nazca plate moves during the time period shorter than a characteristic time $t = \nu/\mu$, where $\nu$ is the effective viscosity and $\mu$ is the elastic rigidity (Nedoma (1998)), by a uniform velocity.

The problem leads to analyse the contact problem with friction in elastic bodies that are subject to body and external forces and that are in mutual contact between several elastic rock bodies. Then the problem leads to solve the variational inequality problem. Numerically the problem represents a FEM approximation of the variational inequality problem and is equivalent to minimize the potentionnal energy over the set of admissible displacements. The numerical results concerning interplate stresses, normal and tangential components displacements and stresses will be discussed.

This research was partially supported by the grant COPERNICUS-HIPERGEOS II-KIT 977006 and by the grant of the Ministry of Education, Youth and Sports of the Czech Republic No OK-407.

---

1991 *Mathematics Subject Classification.* Primary: 86-08, 73T05, 35L85, 73N05,73K25 Secondary: 86A60, 73N10, 90C20, 73C30, 73C60.

*Key words and phrases.* Geodynamics, Andes, subduction of the Nazca Plate beneath the South American Plate, seimology, plate tectonic theory, contact problem with friction, variational inequality problem, finite element method .

## 1. Introduction

The Andean region is located in one of the most seismically active regions in the world. It is the largest region between 10°N and 43°S in which ocean-continent convergence is the present event. The Andes are the result of the subduction of the Nazca Plate beneath the South American plate along the Peru-Chile trench since the Cretaceous. This continental margin orogenic belt is more than 7000km length. It presents distinct broad scale tectonic segments, which correlate with the variations in the geometry of the subducted Nazca plate (Barazangi, Isacks (1976), Jordan et al. (1983)). These segments are conspicous in the Central Andes between 15°S and 27°S. Along the Peru-Chile trench, the subduction of the Nazca Plate under the South American Plate is well underlined by the Wadati-Benioff zone (WBZ).

The WBZ beneath the Andean region has been frequently studied by using the seismic activity (Figs 1a,b,c) and the plate tectonic theory. Isacks, Molnar (1971), Barazangi, Isacks (1976),(1979), Sacks (1977), Smalley, Isacks (1987) and Rodriguez, Tavera (1991), Berrocal, Fernandes (1996) indicate the existence of specific features in the Nazca slab beneath the Andean region, namely the changes of the WBZ dip, having an almost flat behaviour under central and northern regions of Peru and central region of Chile/NW Argentina.

The WBZ beneath the southern Peru and northern Chile region was analysed through data collected by local seismographic networks (Hasegawa, Sacks (1981), Grange et al. (1984), Boyd et al. (1984)). These analyses confirmed the foregoing results of Barazangi, Isacks (1979) of a WBZ with a gently dip in central Peru and a steep dip slab (~30°) in its southern portion. Comte, Suarez (1994), Comte et al. (1994) indicate phase transformation along the slab with normal and reverse faulting at arround 100km and 200km of depth. Delouis et al. (1996) determined a WBZ with a seismically coupled plate interface and localised reverse faults among 20-50km depth with variable azimuth up to 80km depth and with constant azimuth NNW to NW, below it, until 250km. The rotation of the stress axes by relating the deeper portion of the slab is observed.

The seismic activity among 70-300-500km of depth and the concentration of the deep earthquakes in relatively narrow zones oriented almost in the N-S direction was useful for important information to determine the mechanical properties and the stress distribution of the descending slab. Due to Billington and Isacks (1975) and Beck et al. (1995) the determination of the physical mechanism of deep earthquakes is a fundamental problem in seismology. But there are important controversies about the seismotectonic characteristics in the Andean region, in relation both to the morphology of the Wadati-Benioff zone, all along the interaction regions between the plates (see e.g. Cahill, Isacks (1992), Berrocal, Fernandes (1996)).

The aim of this paper is to present certain mathematical model of Andes presented on two profiles - profile S2 across the Villarica volcano and profile S10B across the Peru-Chile border (Figs 2b and 2k). The model will be based on the observation of epicentres of earthquakes (see Engdahl et al. (1997), Berrocal, Fernandes (1996)) and on the shape of the WBZ (fig. 3) as well as on the analyses of the deep faults together with a spatial distribution of volcanoes (Fig.4) (see Dewey,Lamb (1992), López-Escobar et al. (1995)) . Moreover, knowledge about movements of both global lithospheric plates as well as of their subblocks are very important information for mathematical modelling and mathematical simulation

of plate tectonic processes in the region studied. On the other hand, the numerical analyses will bring new information and understanding about tectonic processes taking place in the Andean region, namely the interplate stresses and ascismic zones observed on the WBZ.

## 2. The model.

Since the geodynamical processes taking place in the lithosphere of the Andean region and in the upper mantle during the whole evolutionary geological epoch continue from the Tertiary up to the present, thus the mathematical model of the subduction of the Nazca Plate beneath the South American lithospheric plate must be derived from the mathematical global plate tectonic model (Nedoma (1982), (1986a-c), (1990a,b,c), (2000)), which will be as follows:

Let $0, x_1, ..., x_N$ be the orthogonal Cartesian coordinate system, where $N$ is the space dimension and let $\mathbf{x} = (x_1, ..., x_N)$ be a point in this Cartesian system. Let the lithosphere and the upper mantle, being in an initial stress-strain state and created by a system of elastic anisotropic or isotropic lithospheric plates or geological blocks, respectively, occupy a region $\Omega$. Let $\Omega$ be the region in $\mathbb{R}^N, N = 2, 3$, with a sufficiently smooth boundary $\partial\Omega$. Moreover, we shall assume that $\Omega = \cup_{\iota=1}^{s}\Omega^\iota$. Let the boundary $\partial\Omega$ be divided into disjoint parts $\Gamma_\tau, \Gamma_u, \Gamma_c$ and $\Gamma_0$ such that $\partial\Omega = \Gamma_\tau \cup \Gamma_u \cup \Gamma_c \cup \Gamma_0$, where the parts $\Gamma_\tau, \Gamma_u, \Gamma_c$ and $\Gamma_0$ are open sets in $\partial\Omega$ . Assume that Lamé coefficients $\lambda$ and $\mu$ as well as anisotropic elastic coefficients $c_{ijkl}$ are bounded functions. We then shall assume that $\lambda^\iota, \mu^\iota, c^\iota_{ijkl} \in C^1(\overline{\Omega^\iota})$. Let $I = (t_0, t_1)$ be a time interval, $\Omega_t = \Omega \times I, \partial\Omega_t = \partial\Omega \times I$. Let $\mathbf{u} = \mathbf{u}(\mathbf{x}, t)$ be the displacement vector. Let us denote the outward unit normal to the boundary $\partial\Omega$ by $\mathbf{n} = (n_i)$. The equations of motion for every subdomain $\Omega^\iota$ of $\Omega$ read as follows:

(1) $\rho^\iota \frac{\partial^2 u_i^\iota}{\partial t^2} - \frac{\partial}{\partial x_j}(c^\iota_{ijkl} e_{kl}(\mathbf{u}^\iota)) = F_i^\iota,\ i, j, k, l = 1, ..N,\ (\mathbf{x}, t) \in \Omega_t^\iota,$

which for the case, if the lithospheric plate or geological blocks move during relatively short geological period by an uniform velocity (then we will speak about the quasi-dynamic case), leads to the form

(1a) $\frac{\partial \tau_{ij}(u^\iota)}{\partial x_j} + F_i^\iota = 0,\ i, j = 1, .., N, \iota = 1, .., s,$ in $\Omega_t^\iota$,

where $\mathbf{F}^\iota$ are body forces. A repeated index implies summation from 1 to N.

The relation between the displacement vector $\mathbf{u} = (u_i), i = 1, ..., N$, and the small strain tensor $e_{ij}$ is defined by

(2) $e_{ij} = e_{ij}(\mathbf{u}) = \frac{1}{2}(\frac{\partial u_i}{\partial x_j} + \frac{\partial u_j}{\partial x_i}), i, j = 1, ..., N.$

The relation between the stress and strain tensors is defined by the Hooke's law

(3) $\tau^\iota_{ij} = c^\iota_{ijkl} e_{kl}(\mathbf{u}^\iota),\ i, j, k, l = 1, ..., N, \iota = 1, ..., s,$

in the anisotropic case, whereas in the isotropic case

(4) $c^\iota_{ijkl} = \mu^\iota(\delta_{ik}\delta_{jl} + \delta_{il}\delta_{jk}) + \lambda^\iota \delta_{ij}\delta_{kl},$

where $\lambda^\iota, \mu^\iota$ represent the Lamé coefficients. The coefficients $c^\iota_{ijkl}$ form a matrix of the type $(N \times N \times N \times N)$ and satisfy the symmetry conditions

(5) $c^\iota_{ijkl} = c^\iota_{jikl} = c^\iota_{klij} = c^\iota_{ijlk}$

and

(6) $0 < a_0^\iota \le c^\iota_{ijkl}(\mathbf{x})\xi_{ij}\xi_{kl} \mid \xi \mid^{-2} \le A_0^\iota < +\infty$ for a.e.$\mathbf{x} \in \Omega^\iota$,

$\quad : \xi \in \mathbb{R}^{N^2}, \xi_{ij} = \xi_{ji},$

where $a_0^\iota, A_0^\iota$ are constants independent of $\mathbf{x} \in \Omega^\iota$ and for the isotropic case $a_0^\iota = 2\min\{\mu^\iota(\mathbf{x}); \mathbf{x} \in \Omega^\iota\}$ and $A_0^\iota = \max\{2\mu^\iota(\mathbf{x}) + 3\lambda^\iota(\mathbf{x}); \mathbf{x} \in \Omega^\iota\}$.

We shall consider the condition of loading on the Earth surface $\Gamma_\tau$ in the form

(7) $\tau_{ij}n_j = P_i$ on $\Gamma_\tau \times I$.

Let the boundary $\Gamma_u = {}^1\Gamma_u \cup {}^2\Gamma_u$. Let us assume that a portion of the examined geological body does not move at a certain part of boundary which will be denoted by ${}^1\Gamma_u$. We thus have e.g. the conditions

(8) $u_i = {}^1u_{0i}$ $(= 0)$ on ${}^1\Gamma_u \times I$.

Furthermore, we can simulate the movement of an invasing plate by the displacement vector given at the boundary ${}^2\Gamma_u$

(9) $u_i = {}^2u_{0i}$ $(\neq 0), i = 1, ..., N$, on ${}^2\Gamma_u \times I$.

Assume that the investigated Andean region $\Omega$ consists of $s$ lithospheric plates and blocks $\Omega^\iota, \iota = 1, ..., s$, so that $\Omega = \cup_{\iota=1}^{s}\Omega^\iota$, and let several neighbouring plates or geological blocks (we will speak about geological bodies), say $\Omega^k$ and $\Omega^l$, are in a mutual contact. Denote the common contact boundary between both geological bodies $\Omega^k$ and $\Omega^l$ before deformation by $\Gamma_c^{kl}$. Let us denote the outward unit normal to the contact boundary $\Gamma_c^{kl}$ by $\mathbf{n} = (n_i)$. Let $\mathbf{t} = (t_i)$ be the unit tangential vector to the contact boundary $\Gamma_c^{kl}$. Further, denote by $\tau_i = \tau_{ij}n_j$ the stress vector, its normal and tangential components by $\tau_n = \tau_i n_i = \tau_{ij}n_i n_j, \boldsymbol{\tau}_t = \boldsymbol{\tau} - \tau_n \mathbf{n}$, and the normal and tangential components of displacement vector by $u_n = u_i n_i$ and $\mathbf{u}_t = \mathbf{u} - u_n \mathbf{n}$. Denote by $\mathbf{u}^k, \mathbf{u}^l$ (indices $k, l$ correspond with the neighbouring geological blocks in contact) the displacements in the neighbouring blocks. All these quantities are functions of spatial coordinates. Then on the contact boundaries $\Gamma_c^{kl}$ the condition of non-penetration

(10) $u_n^k - u_n^l \leq 0$ on $\Gamma_c^{kl} \times I$

holds.

For the contact forces, due to the law of action and reaction, we find

(11) $\tau_n^k = -\tau_n^l \equiv \tau_n^{kl}, \boldsymbol{\tau}_t^k = -\boldsymbol{\tau}_t^l \equiv \boldsymbol{\tau}_t^{kl}$.

Since the normal components of contact forces cannot be positive, i.e. cannot be tensile forces, then

(12) $\tau_n^k = -\tau_n^l \equiv \tau_n^{kl} \leq 0$ on $\Gamma_c^{kl} \times I$.

During the deformation of the geological bodies they are in contact or they are not in contact. If they are not in contact, then $u_n^k - u_n^l < 0$, and the contact forces are equal to zero, i.e. $\tau_n^k = -\tau_n^l \equiv \tau_n^{kl} = 0$. If the geological bodies are in contact, i.e. $u_n^k - u_n^l = 0$, then there may exist non zero contact forces $\tau_n^k = -\tau_n^l \equiv \tau_n^{kl} \leq 0$. These cases are included in the following condition

(13) $(u_n^k - u_n^l)\tau_n^{kl} = 0$ on $\Gamma_c^{kl} \times I$.

Further, if both geological bodies are in contact, then on the contact boundary the Coulombian type of friction acts. The frictional forces $g_c^{kl}$ acting on the contact boundary $\Gamma_c^{kl}$ are, in their absolute value, proportional to the normal stress component, where the coefficient of proportionality is the coefficient of Coulombian friction $\mathcal{F}_c^{kl}$, i.e.

(14) $g_c^{kl} = \mathcal{F}_c^{kl} \mid \tau_n^{kl} \mid$.

Due to the acting frictional forces we have the following cases:

If the absolute value of tangential forces $\boldsymbol{\tau}_t^{kl}$ is less than the frictional forces $g_c^{kl}$, then the frictional forces preclude the mutual shifts of both geological bodies being in contact. If the tangential forces $\boldsymbol{\tau}_t^{kl}$ are equal in their absolute value to the frictional forces, so that are no forces which can preclude the mutual, i.e. bilateral, motion of both geological bodies. Thus the contact points change their position in the direction opposite to that in which the tangential stress component acts. These facts are described by the following conditions:

(15a) if $u_n^k - u_n^l = 0$ then $\mid \boldsymbol{\tau}_t^{kl} \mid \leq g_c^{kl}$

(15b) if $|\tau_t^{kl}| < g_c^{kl}$ then $\mathbf{u}_t^k - \mathbf{u}_t^l = 0$,

which means that the friction forces are sufficient to preclude the mutual shifting between the assumed bodies and

(15c) if $|\tau_t^{kl}| = g_c^{kl}$ then there exists a function $\vartheta \geq 0$ such that

$$: \mathbf{u}_t^k - \mathbf{u}_t^l = -\vartheta \tau_t^{kl},$$

which means that the friction forces are not sufficient to preclude the mutual-bilateral shifting of both assumed geological bodies. This shift acts in an opposite direction to the acting tangential forces.

When $\mathcal{F}_c^{kl} = 0$ then $g_c^{kl} = 0$ and then $\tau_t^k = -\tau_t^l = 0$, and we speak about the case of contact problems without friction. In the case if $s = 1$, i.e. if the second body is approximated by an absolutely rigid material and the frictional forces are equal to zero, then Eqs (10),(12),(13) reduce to

(16) $u_n \leq 0, \tau_n \leq 0, u_n \tau_n = 0.$

In some problems the conditions of symmetry

(17) $u_n = 0, \tau_{tj} = 0,\ j = 1, ..., N$

can be used on the axis (or plane) of symmetry. This type of conditions is useful namely for 3D model problems.

The amplitude of the Coulombian coefficient of friction is not known, but for the existence of a solution it can be estimated (see Hlaváček et al. (1988), Haslinger et al. (1996), Jarušek (1983) for the elastic case and Nedoma (1987),(1998) for the thermo-elastic case) e.g. for the isotropic case by

(18) $\| \mathcal{F}_c^{kl} \| < (c_s/c_p)^{\frac{1}{2}}$,

where $c_s$ and $c_p$ are the velocities of S and P seismic waves. We see that the coefficient of friction depends on the material properties only.

**Remark 2.1.** *We say that the problem investigated will be coercive if $\Gamma_u^\iota \neq \emptyset$ for all $\iota = 1, ..., s$ and semi-coercive if at least one part of $\Gamma_u = \cup_{\iota=1}^s \Gamma_u^\iota$, say $\Gamma_u^\jmath$, is empty.*

## 3. Numerical Solution of the Problem

To solve the problem numerically we derive its variational (weak) solution. Assume that the domain $\Omega$ is occupied by the Nazca and South American plates, which are assumed to be isotropic or anisotropic, and moving by an uniform velocity during the investigated short (from the geological point of view) time period and that Lamé coefficients $\lambda$ and $\mu$ as well as anisotropic elastic coefficients $c_{ijkl}$ are bounded functions. In the following for our analyzes of the subduction of the Nazca Plate beneath the South Americal Plate we shall consider the 2D semi-coercive quasi-dynamic case (Nedoma (1994), (1998)).

Let $\Omega \subset \mathbb{R}^N, N = 2, 3$ be a union of domains, occupied by a geological bodies, with a sufficiently smooth boundaries $\partial\Omega^\iota$, consisting of three parts $\Gamma_\tau, \Gamma_u, \Gamma_c$, $\partial\Omega = \Gamma_\tau \cup \Gamma_u \cup \Gamma_c$, all defined above. Let $\mathbf{x} = (x_i), i = 1, 2, (3)$ be the Cartesian co-ordinates and let $\mathbf{n} = (n_i)$, $\mathbf{t} = (t_i) = (-n_2, n_1)$ be the outward normal and tangential vectors to $\partial\Omega$. Let us look for the displacement vector $\mathbf{u} = (u_i) \in \mathbf{W}(\Omega) = [H^1(\Omega)]^N$, where $H^1(\Omega)$ is the Sobolev space in the usual sense (see Nedoma (1998)). Let $e_{ij}(\mathbf{u}), \tau_{ij}(\mathbf{u})$ be the small strain tensor and the stress tensor, respectively, and $\rho^\iota = \rho^\iota(\mathbf{x}) \in C(\overline{\Omega}^\iota)$ the density. Let for every time $t$ components of body forces $F_i \in L^2(\Omega)$,components of surface forces $P_i \in L^2(\Gamma_\tau)$and coefficients of elasticity $c_{ijkl}^\iota \in C^1(\overline{\Omega}^\iota)$ satisfy the usual symmetry conditions and the usual ellipticity and continuity conditions. Let $g_c^{kl} \in L^2(\Gamma_c^{kl})$ be given slip limits.

Let us denote by $(.,.)$ the scalar product in $[L^2(\Omega)]^N$, by $<.,.>$ the scalar product in $[L^2(\Gamma_c)]^N$, by $\| \cdot \|_k$ the norm in $[H^k(\Omega)]^N$, $k$ being an integer, where $H^k(\Omega)$ denotes the Sobolev space in the usual sense. Let us denote by

$V_0 = \{\mathbf{v} \mid \mathbf{v} \in \mathbf{W} \equiv [H^1(\Omega^1)]^N \times .. \times [H^1(\Omega^s)]^N, \mathbf{v} = 0 \text{ on } {}^1\Gamma_u \cup {}^2\Gamma_u\}$

$V = \{\mathbf{v} \mid \mathbf{v} \in \mathbf{W}, \mathbf{v} = \mathbf{u}_0 \text{ on } {}^1\Gamma_u \cup {}^2\Gamma_u\}$

the spaces and sets of virtual displacements, respectively, and by

$K = \{\mathbf{v} \mid \mathbf{v} \in V, v_n^k - v_n^l \leq 0 \text{ on } \cup_{k,l}\Gamma_c^{kl}\}$

the set of all admissible displacements.

Multiplying (1a) by $\mathbf{v} - \mathbf{u}$, integrating over $\Omega$ for all $t$ (we will use the notation $\forall t$) from the investigated geological time period, using the divergence theorem and boundary conditions, then we have to solve the following variational problem:

we will find function $\mathbf{u} \in K$ $\forall t$, such that

(19) $a(\mathbf{u}, \mathbf{v} - \mathbf{u}) + < g_c^{kl}, \mid \mathbf{v}_t^k - \mathbf{v}_t^l \mid - \mid \mathbf{u}_t^k - \mathbf{u}_t^l \mid > \geq S(\mathbf{v} - \mathbf{u})$ $\forall \mathbf{v} \in K$ $\forall t$,

where for $\mathbf{u}, \mathbf{v} \in \mathbf{W}$ we put

$a(\mathbf{u}, \mathbf{v}) = \sum_{i=1}^{s} a(\mathbf{u}, \mathbf{v}) = \int_\Omega c_{ijkl} e_{ij}(\mathbf{u}) e_{kl}(\mathbf{v}) d\mathbf{x}$,

$S(\mathbf{v}) = \sum_{i=1}^{s} S^i(\mathbf{v}^i) = \int_\Omega F_i v_i d\mathbf{x} + \int_{\Gamma_\tau} P_i v_i ds$,

$j_{gn}(\mathbf{v}) = \int_{\cup_{k,l}\Gamma_c^{kl}} g_c^{kl} \mid \mathbf{v}_t^k - \mathbf{v}_t^l \mid ds = < g_c^{kl}, \mid \mathbf{v}_t^k - \mathbf{v}_t^l \mid >$ .

The problem (19) represents the variational inequality and is equivalent to the following variational formulation:

Find a function $\mathbf{u} \in K$ $\forall t$, such that

(20) $L(\mathbf{u}) \leq L(\mathbf{v})$ $\forall \mathbf{v} \in K$ $\forall t$,

where $L(\mathbf{v})$ is defined by

(21) $L(\mathbf{v}) = L_0(\mathbf{v}) + j_{gn}(\mathbf{v})$, $L_0(\mathbf{v}) = \frac{1}{2} a(\mathbf{v}, \mathbf{v}) - S(\mathbf{v})$,

which means that we minimize the functional of potential energy $L(\mathbf{v})$ on the set of all admissible displacements (while in the case of the classical BVP in elasticity we minimize the functional of potential energy on the space of all virtual displacements).

To prove the existence and uniqueness of the variational (weak) solution we introduce the set of all rigid displacements and rotations

$P = \cup_{i=1}^{s} P^i$, where for $N = 3$ $P^i = \{\mathbf{v} \mid \mathbf{v} \in [H^1(\Omega^i)]^3, \mathbf{v} = \mathbf{a}^i + \mathbf{b}^i \times \mathbf{x}\}$ and

for $N = 2$ $P^i = \{\mathbf{v}^i \mid \mathbf{v}^i = (v_1^i, v_2^i) \in [H^1(\Omega^i)]^2, v_1 = a_1^i - b^i x_2, v_2 = a_2^i + b^i x_1\}$,

where $\mathbf{a}^i, \mathbf{b}^i$ are arbitrary real vectors for $N = 3$ or $b^i$ are arbitraly real scalars for $N = 2$.

Then we can find that there exists a weak solution of the problem under the condition

(22) $S(\mathbf{w}) \leq j_{gn}(\mathbf{w})$ $\forall \mathbf{w} \in K \cap P$, i.e.

$$: \int_\Omega F_i w_i d\mathbf{x} + \int_{\Gamma_\tau} P_i w_i ds - \int_{\cup_{k,l}\Gamma_c^{kl}} g_c^{kl} \mid \mathbf{w}_t^k - \mathbf{w}_t^l \mid ds \leq 0$$

$$: \forall \mathbf{w} \in K \cap P,$$

representing the necessary condition for the existence of the solution (Nedoma, 1998a).

**Finite Element Solution of the Problem**

Let the domain $\Omega \subset \mathbb{R}^N$ be a bounded domain and let it be approximated by a polygonal (for $N = 2$) or polyhedral (for $N = 3$) domain $\Omega_h$. Let the domain $\Omega_h$ be "triangulated", i.e. the domain $\bar{\Omega}_h = \Omega_h \cup \partial\Omega_h$ is divided into a system of $m$ triangles $T_{h_i}$ in the 2D case and into a system of $m$ tetrahedra $T_{h_i}$ in the 3D case, generating a triangulation $\mathcal{T}_h$ such that $\bar{\Omega}_h = \cup_{i=1}^{m} T_{h_i}$ and such that two neighbouring triangles have only a vertex or an entire side common in the 2D

case, and that two neighbouring tertrahedra have only a vertex or an entire edge or an entire face common in the 3D case. Denote by $h = \max_{1\le i\le m}(diam\ T_{h_i})$ the maximal side of the triangle $T_{h_i}$ in the 2D case and/or the maximal edge of the tetrahedron in the 3D case in $\mathcal{T}_h$. Let $\rho_{T_i}$ denote the radius of the maximal circle (for 2D case) or maximal ball (for 3D case), inscribed in the simplex $T_{h_i}$. A family of triangulation $\{\mathcal{T}_h\}, 0 < h \le h_0 < \infty$, is said to be regular if there exists a constant $\vartheta_0 > 0$ independent of $h$ and such that $h/\rho_{T_i} \le \vartheta_0$ for all $h \in (0, h_0)$. We will assume that the sets $\bar\Gamma_u \cap \bar\Gamma_\tau$, $\bar\Gamma_u \cap \bar\Gamma_c$, $\bar\Gamma_u \cap \bar\Gamma_0$, $\bar\Gamma_c \cap \bar\Gamma_\tau$, $\bar\Gamma_c \cap \bar\Gamma_0$, $\bar\Gamma_\tau \cap \bar\Gamma_0$ coincide with the vertices or edges of $T_{h_i}$.

Let $R_i \in \Omega_h$ be an arbitrary interior vertex of the triangulation $\mathcal{T}_h$. Generally the basis function $w_h^i$ (where $w_h^i$ is a scalar or vector function) is defined to be a function linear on each element $T_{h_i} \in \mathcal{T}_h$ and taking the values $w_h^i(R_j) = \delta_{ij}$ at the vertices of the triangulation, where $\delta_{ij}$ is the Kronecker symbol. The function $w_h^i$ represents a pyramid of height 1 with its vertex above the point $R_i$ and with its support (supp $w_h^i$) consisting of those triangles or tetrahedra which have the vertex $R_i$ in common. The basis function has small support since $diam(\text{supp } w_h^i) \le 2h$ and the parameter $h \to 0$. Further, for simplicity, we shall discuss the 3D case, where all physical parameters will be independent of the $x_2$ co-ordinate only. Such problems lead to solving the 2D model problems only (Nedoma (1983), (1987),(1998)).

Let us assume that $N = 2$. Let $V_h$ be the spaces of linear finite elements, i.e. the spaces of continuous vector functions in $\bar\Omega_h$, piecewise linear over $\mathcal{T}_h$, i.e.

$V_h = \{\mathbf{v} \in [C(\bar\Omega_h^1)]^2 \times .... \times [C(\bar\Omega_h^s)]^2 \cap V \mid \mathbf{v}_{|T_{h_i}} \in [P_1]^2\ \forall T_{h_i} \in \mathcal{T}_h\}$

and

$K_h = \{\mathbf{v} \in V_h \mid v_n^k - v_n^l \le 0 \text{ on } \cup\Gamma_c^{kl}\} = K \cap V_h$.

A function $\mathbf{u}_h \in K_h$, is said to be a finite element solution of the model problem studied, if

(23) $L(\mathbf{u}_h) \le L(\mathbf{v})\ \forall \mathbf{v} \in K_h$,

which is equivalent to minimize the FEM approximation of the functional of potential energy over the approximation of the set of all admissible displacements $K_h$.

To find an apriori estimate for the error of the solution $\mid \mathbf{u}_h - \mathbf{u} \mid$,where $\mathbf{u}$ is an exact solution and $\mathbf{u}_h$ is a FEM solution of the model problem, then using modification the Falk's technique, we find (see Nedoma (1998)) that under the certain assumptions $\mid \mathbf{u} - \mathbf{u}_h \mid = O(h), h \to 0_+$.

Finite element technique used requires the solution of the contact problem with friction by using the numerical approximation of a saddle point. By an approximation of a saddle is meant a point $(\mathbf{u}_{sh}, \lambda_h) \in K_h \times \Lambda_h$ of a functional $\mathcal{L}$, the so-called Lagrangian, on $K_h \times \Lambda_h$, if a saddle point $(\mathbf{u}_s, \lambda) \in K \times \Lambda$ exists and if

$\mathcal{L}(\mathbf{u}_{sh}, \mu_h) \le \mathcal{L}(\mathbf{u}_{sh}, \lambda_h) \le \mathcal{L}(\mathbf{v}_h, \lambda_h)$

for all pairs of functions $(\mathbf{v}_h, \mu_h) \in K_h \times \Lambda_h$. The problem for a fixed $t$ is equivalent to find $\mathbf{u}_h \in K_h$ such that

(24) $L(\mathbf{u}_h) = \min_{\mathbf{v}_h \in K_h} \sup_{\mu_h \in \Lambda_h} \{\mathcal{L}(\mathbf{v}_h, \mu_h) = L_0(\mathbf{v}_h) + \int_{\cup\Gamma_{ch}^{kl}} \mu_h^{kl} g_c^{kl}(\mathbf{v}_{ht}^k - \mathbf{v}_{ht}^l) ds\}$,

where $\Lambda_h$ is the approximation of the set of the Lagrangian multipliers $\mu^{kl}$, i.e. of the set $\Lambda = \cup\{\mu^{kl} \mid \mu^{kl} \in L^2(\Gamma_c^{kl}), \mid \mu^{kl} \mid \le 1 \text{ a.e. on } \Gamma_c^{kl}\}$, $\mathcal{L}$ is the Lagrangian and where the non-differential functional $j_{gn}(\mathbf{v}) = \int_{\cup\Gamma_c^{kl}} g_c^{kl} \mid \mathbf{v}_t^k - \mathbf{v}_t^l \mid ds$ was replaced by $j_{gn}(\mathbf{v}_h) = \int_{\cup\Gamma_{ch}^{kl}} \mu_h^{kl} g_c^{kl}(\mathbf{v}_{ht}^k - \mathbf{v}_{ht}^l) ds$.

For the numerical realization of a saddle point, the Uzawa algorithm was used. The Uzawa algorithm is as follows:

let us choose $\lambda_h^0 \in \Lambda_h$, e.g. $\lambda_h^0 = 0$. let $\lambda_h^i \in \Lambda_h$ be known, then we find $\mathrm{u} \in K_h$ solving the following problem

(25) $\min_{\mathbf{v}_h \in K_h} \{L(\mathbf{v}_h) = L_0(\mathbf{v}_h) + \int_{\cup \Gamma_{kl}^{kl}} \lambda_h^{i,kl} g_c^{kl}(\mathbf{v}_{ht}^k - \mathbf{v}_{ht}^l) ds\}$,

and $\lambda_h^{i+1,kl} = P(\lambda_h^{i,kl} + \rho_i g_c^{kl}((u_{hi}^k)_t - (u_{hi}^l)_t))$, where $P$ is a projection $P : L^2(\Gamma_c^{kl}) \to \Lambda_h$ defined as follows

$\mu \in L^2(\Gamma_c^{kl}), y \in \Gamma_c^{kl}$,

$P\mu(y) = \mu(y)$ for $\mid \mu(y) \mid \leq 1$,

$P\mu(y) = 1$ for $\mu(y) > 1$,

$P\mu(y) = -1$ for $\mu(y) < -1$,

$\rho > 0, 0 < \rho_1 \leq \rho_i \leq \rho_2, \rho_1, \rho_2$ are sufficiently small numbers following from the convergence theorem of the Uzawa algorithm (see Nedoma (1998)).

Minimization of the functional $L(\mathbf{v}_h)$ over the set of admissible displacements $K_h$ then is equivalent to the problem

(26) $f(\mathbf{w}) = \frac{1}{2}\mathbf{w}^T C\mathbf{w} - \mathbf{b}^T\mathbf{w}$ with linear constraints $A\mathbf{w} \leq \mathrm{d}$,

where in our case the functional $f(\mathbf{w})$ is generated from the functional $L(\mathbf{v}_h)$, $C$ is the stiffness matrix ($\dim n \times m$), which is positive (semi-)definite and generated by the term $\frac{1}{2}\int_\Omega c_{ijkl} e_{ij}(\mathbf{u}) e_{kl}(\mathbf{v}) d\mathbf{x}$; $\mathrm{b}$ ($\dim n$) is the vector generated by the body and surface forces, i.e. by the term $\int_\Omega F_i w_i d\mathbf{x} + \int_{\Gamma_\sigma} P_i w_i ds$ and by the friction forces $\int_{\cup_{k,l}\Gamma_c^{kl}} \mu^{kl} g_c^{kl}(\mathbf{w}_t^k - \mathbf{w}_t^l) ds$ and it changes due to the friction forces in every step of the Uzawa algorithm; $A$ ($\dim m \times n$) is the matrix of constraints generated by the condition of non-penetration $u_n^k - u_n^l \leq 0$ on $\Gamma_c^{kl}$ in the definition of the admissible set of displacements $K_h, \mathbf{d} \equiv \mathbf{0}$.

For solving constrained optimization methods the gradient projection method, like the steepest descent method adapted to constrained optimization problems, can be generally useful. Since the functional $f(\mathbf{w})$ is a quadratic functional, then the conjugate gradient method with linear constraints and with or without preconditioning or the penalized method, the elimination method and the method of dual variables, respectively, can be applied (Daniel (1971), Brousse (1988), Luenberger (1984), Nedoma (1998), Nedoma et al. (1999)).

## 4. Discussions of Results. Conclussion

The results are based on the analysis of the spatial distribution of high quality of earthquake hypocentres, occurred in the Andean region in the period 1964-1995. Moreover, the analysis of the space-time distribution of all data of very deep South American earthquakes is used to define some seismotectonic features beneath the Andean region (Muñoz, Stern (1988), López-Escobar et al. (1995), Berrocal, Fernandes (1996), Engdahl et al. (1997), Giese et al. (1999)). In Figs 1 and 2 the epicentres of earthquakes, that have occurred in the WBZ beneath the Andean region during January 1964 -December 1995, are plotted, where in Fig.1a the epicentres of events with h$\leq$ 50km are plotted, while in Fig.1b the epicentres of events with $h >$ 50km are shown, both to include mainly the activity in the WBZ beneath the Andean region between 0° to 50°$S$ and in Fig.1c and Figs 2a-r their distribution with depth is given. The numerical analysis will be made on two profile across the Andes, which was divided in to 14th sections. We constructed our profiles

crossing the sections S2 and S10B and we will denote our profiles as the profile S2, which acrossing the Villarica volcano and as the profile S10B, which crossing the Peru/Chile border. The profile S2 indicates a dip of arround 20° and a maximum depth of 150km (see Fig.2b).The profile S10B shown in Fig.2k, represents a WBZ with seismic activity up to 300km of depth, followed by a seismic gap up to 550km and then it continuous with the very deep activity up to arround 600km of depth. Section S10B seems to be a best representation of the WBZ in the southern Peru-Peru/Chile border region.

The collision of lithospheric plates represents the actual cause of the large stresses and strains in the lithosphere. The lithosphere thus behaves like a stress guide. Since this process plays an important role in tectonophysics, therefore, we will study this problem in greater details. One of the main goal of this study is to show that the mathematical model of the subduction of Nazca plate below the South American Plate, corresponding to the plate tectonic theory, is more correctly described by variational inequalities (see the previous section) than by the classical approach leading on the variational equalities. Such model problems accurately approximate the mutual shifts of the subducting and obducting plates as well as their parts - geological blocks, along common contact boundaries or along the common boundary between the lithosphere and the asthenosphere, wholly in the sense of theplate tectonic hypothesis. On the contrary, the classicalapproach based on BVPs in the theory of elasticity (visco-elasticity) corresponds to the static models of the crust or a partof the lithosphere resting on their support, which do not render their mutual shifting.

In our approach we will assume that the present relative movements of the invasing Nazca Plate is of about 10 cm/yr, while the present relative movements of the South American Plate in its central part is of about 2.5cm/yr, which corresponds to the relative motion 5cm/yr of the spreading of Atlantic oceanic lithosphere. Moreover, we will assume that the investigated geological time interval will be the sum of time intervals, which are shorter than the characteristic time $t_c$ for which the lithosphere behaves as an elastic medium. In a real lithosphere and the upper parts of the mantle and for a longer geological time periods a non-linear creep represents the dominant mechanism. Then the upper parts of the Earth will be approximated by the visco-elastic or visco-plastic model problems. But in our study, for simplicity, we will study the behaviour of the upper parts if the Earth during very short (from the geological point of view) geological time period and, moreover, we will assume that during this time the Nazca Plate moves by the uniform velocity 10cm/yr. The models corresponding to the profile S2 - Villarica volcano and the profile S10B across the Peru/Chile border are based on the seismotectonic results of Engdahl et al. (1995), Berrocal, Fernandes (1996), Kirchner et al. (1996). The models - profiles S2 and S10B, assume a lithospheric plates of 80-100km thick, with densities between 2500-3400kgm$^{-3}$, velocities of seismic P-waves between 6100-8120 msec$^{-1}$ and velocities of seismic S-waves between 3540-4690 msec$^{-1}$. The surface confoguration was obtained from the distribution of intermediate and deep earthquakes as well as of a situation of deep faults.

In order to model problems of both investigated sections S2 and S10B, we will apply the theory derived in Nedoma (1998), and which is shortly presents in the previous section, for a limited part of the South American continental lithospheric plate, the Nazca Plate and the upper mantle, we have to improve boundary conditions on the plate limits. These conditions replace the relative motion of both

lithospheric plates at greater distances from the subduction zone. Furthermore, we assume that the Earth's surface is load free. At greater depth under the lithosphere we will assume that on these surfaces the displacements are very small, practically equal to zero.

In order to give the equations of motion we shall assume that both lithospheric plates and the upper mantle are formed by inhomogeneous isotropic materials and that the variability in time of the body and surface forces are slow, and moreover, that the motion of the lithospheric plates is uniform over the last several million years (from which we will investigate from the geological point of view a small time interval only). Then the problem can be studied as quasi-stationary and elastic one and the inerti forces can be neglected. In our nmerical study we will limit ourselves to the 2D case only. The lithosphere is modelled by a non-homogeneous and broken up medium resting with friction over the asthenosphere and subducted to the upper mantle.

The main results are illustrated in Figs 5-12 for the geological time interval 1000yrs. In Fig.5 the geometry of the model problem corresponding to the profile S2 across the volcano Villarica is presented. The numbers in Fig.5 represent contact points lying in the subduction zone, on the common boundary of the Nazca Plate and the South American plate and their common boundaries with the upper mantle (the mesosphere). In Figs 6a-h the interplate stresses in Pa are illustrated. In Fig.6a the principal stresses in the whole studied region is presented, while in Figs 6b-e their details (zooms) are given. In Figs 6f-h the stress tensor components $\tau_{xx} \equiv s_x, \tau_{xz} \equiv s_{xz}, \tau_{zz} \equiv s_z$ are given. Their analyses indicate accumulation of stresses in three main areas (see Figs 6a-h) and between them the areas with a great drop of stresses, which can be indicated both from the principal stresses as well as from the components of stress tensor $(s_x, s_{xz}, s_z)$. On the results of Figs 6b-e one can better to analyse the type of stresses, where —><— represents compression and <——> represents extension, and then we can to say something about the mechanism of earthquakes observed in these region, which will correspond to the mechanism known from the fracture mechanics . But one can alos analyse the other type of earthquake mechanism (see Nedoma (1998),pp. 503-507). We saw in section 2 that on the contact boundaries between collidied lithospheric plates and blocks, we denoted them by $\Gamma_c^{kl}$, the Coulombian friction acts. Then the analysis of the earthquake mechanism is based on numerical analysis of the contact conditions (10)-(15) at every time level $t_i \in \langle t_0, t_1 \rangle$. For detailed analysis see Nedoma (1998), Chapters 7 and 8. That is to say that if the absolute value of the tangential stresses is less than the frictional forces acting on the common contact boundaries, then the tangential force precludes the mutal motion of both colliding blocks or plates, where the frictional forces (we denote them by $g_c^{kl}$) are in their absolute value proportional to the normal stress component, where the coefficient of proportionality is the coefficient of Coulombian friction $\mathcal{F}_c^{kl}$, i.e. $g_c^{kl} \equiv \mathcal{F}_c^{kl} \mid \tau_n^{kl} \mid$ . In this case the deformation energy further accumulates. If the absolute value of the tangential stresses reach the value of frictional forces $g_c^{kl}$, then there are no forces which can preclude the mutual shifting of both colliding geological bodies, i.e. lithospheric plates and geological blocks. Thus the contact points shifts in the direction opposite to that in which the tangential stress component acts. At the same time one part of the deformation energy, accumulated in the subduction zone and its neighbouring regions, is released in the form of the earthquakes. These conclusions are valid for investigations during very short time intervals and can be determined from

the $\tau_n \div \tau_t$ dependence. These studies are out of our present interests, since the present software does not facilitate such studies. The diagrams of normal/tangential components of displacement vector and the stress vector are presented in Figs 7 and 8. From the graph of $u_n$ on the contact boundaries in the subduction zone (numbers no 85÷53) and between the South Americanlithospheric plate and the asthenosphere (numbers no 53÷43) we see that in the subduction zone two bulged out areas occur, while on the contact boundary with the asthenosphere (points No 51(53)÷39, we numbered points on the contact boundaries from the both sides so that the contact point No 51 is the opposite contact point to the one of No 53) normal component of displacement vector is equal to zero, so that we can identify the shift of the invasing Nazca Plate and its sinking in the subduction zone per investigated time interval (i.e. between points No 51 and No 21). Since the temperature of melting depends on the pressure and temperature, then if the pressure increases the temperature of melting also increases, it it decreases then the temperature of melting also desreases. Since the pressure falss in the areas when the normal component of displacement vector is nonzero (i.e. points No 219 and No 213 and their close neighbourhoods) the rocks are melted or partially melted (created the so-called magma), the gases are quickly released, resulting the volcano chambers. We can indicate the volcanic chamber of the volcano Villarica in the depth of about 60 km and in the distance 100kmfrom the Peru-Chile trench. The normal component of the displacement vector indicates the size and the shape of volcanic chambers during the investigated time interval. The tensile stresses in figure Fig. 6a indicate the places of deep faults. Rocks absorb gases, which after their release from the rocks, compress the magma, and then transport it along these deep faults up to the place of the Earth's surface, where the volcanoes Villarica, Quetrupillán and Lanín are situated. The rocks up to a certain distances from these anomalous geothermal regions are also recrystallized and/or metamorphosed. These anomalous geothermal regions are result of the above mechanismas as well as of the effect of dissipation of deformation energy into a heat and of the change of the frictional effect into a heat.

In Fig.9 the geometry of the model corresponding to the profile of the section S10B is presented. Similarly as in the previous case the numbers represent contact points lying in the subduction zone of the Nazca Plate and the South American Plate and their common boundary with the asthenosphere. In Figs 10a-g the distributions of stress field in the studied region is presented. In Figs 10a-d the principal stresses in the whole region studied as well as their zooms are given. In Figs 10e-g the stress tensor components $s_x$, $s_{xz}$, $s_z$, corresponding to the time interval 1000yrs, are illustrated. Analysing Figs10a,b we elliminate places where stresses are accumuilated; the first one is situated at the depth of about 22km and in the distance approximatelly 42km from the Peru/Chile trench; the second one is situated at the depth of about 175 km and in the distance from the Peru/Chile trench of about 330km and the third one at the depth of about 590km and in the distance from the Peru/Chile trench of about 1000km, where the maximal compression is observed and in the depth of about 610km and the distance from the Peru/Chile trench 993km as well as in the depth of about 587km and the distance from the Peru/Chile trench of about 1015km, where extensions are observed. Between them the aseismic zones are observed (see Fig. 10a). Similarly as in the previous Villarica volcano case we can analyse the type of earthquake mechanism (compression

versus extension) and compare with the observed earthquakes. In Figs 10e-f representing stress tensor components we can elliminate similar conclusions as in the Villarica volcano case. Figs 11a,b and 12a,b illustrate normal and tangential components of displacement and stress vectors. In Fig. 11a we indicate 5 places on the sinking lithosphere (contact points No 93 - No 83) in the subducting zone and two on the contact boundary with the asthenosphere (contact points No 83 - No 77) where the normal component of displacement vector $u_n$ is non-zero, but its absolute value over the investigated time interval is relatively small, approx. 100 times smaller than in the Villarica volcano case, which is in the relation of the very deep subduction of the Nazca Plate below the South American Plate. The tangential component of displacement vector describes the mutual movements in the subduction zone as well as on the contact boundary with the asthenosphere. Figs 12a,b illustrate normal and tangential components of stress vector. Their analysis indicate greater values of normal stress component with great peaks at the point No 83 with coordinates (268km,140km), No 80 with coordinates (440km,108km) lying between contact points No 83 and No 78 and No 279 lying near the contact point with coordinates (768km,100km) (see Fig.12a) and at the contact point No 34 with coordinates (980km,612km) lying in the lower part of the subducted lithosphere and with the value of compression of about $-2.10^{10}$Pa, while the maximal value of compression in the contact point No 83 is approx. $-6.10^{9}$Pa. Smaller values of normal displacement component in the case of the profile S10B have connection with very deep subduction of the Nazca Plate below the South American Plate. On the opposite side the normal stresses are of one order greater than in the Villarica volcano case. It is really too interesting that the contacty boundary of the sinking Nazca Plate and the surroundings (vicinity) and the bottom of the South American lithosphere and the neighbouring asthenosphere are partially melted or in the local places are melted; the mechanism of which is of the same type as in the Villarica volcano case.

## References


[1] Barazangi,M., Isacks, B.L. (1976). Spatial distribution of earthquakes and subduction of the Nazca Plate beneath South America. Geology, 4,686-692.

[2] Barazangi, M., Isacks, B.L. (1979). Subduction of the Nazca Plate beneath Peru: evidences from spatial distribution of earthquakes. Geophys.J.R. astron. Soc. 57,537-555.

[3] Beck, S.L., Wallace,T.C, James,D. (1995). Directivity analysis of deep Bolivian earthquake of June 1994. Geophys. Res. Lett. 22,2257-2260.

[4] Berrocal,J., Fernandes,C. (1996). Seismotectonic Features of the Wadati-Benioff zone in the Andean region. Proc. 3rd ISAG, St Malo (France), 17-19.9.1996.

[5] Berrocal,J., Fernandes,C. (1996). Seismotectonic features of the Wadati-Benioff zone in the Andean region. In: Special Issue "Andean Tectonics".

[6] Berrocal,J., Nedoma,J., Kestřánek,Z. (2000). Numerical modelling of tectonic evolution of the Wadati-Benioff zone beneath teh Andean region. Proc.16th World Congress, Lausanne.

[7] Billington,S., Isacks,B.L., (1975). Identification of fault planes accociated with eep eartqankes. Geophys. Res.Lett., 2,63-66.

[8] Boyd,T., Snoke,A., Sacks,I.S., Rodriguez,Z.A. (1984). High resolution determination of the Benioff zone geometry beneath southern Peru. Bull. Seimol. Soc. Am., 74,557-566.

[9] Brouse,P. (1988). Optimization in Mechanics: Problems and Methods. North-Holland, Amsterdam, New York, Oxford, Tokyo.

[10] Cahill,T., Isacks,B.L. (1992). Seismicity and shape of the subducted plate. J.Geophys. Res., 97,17.503-17.529.

[11] Comte,D., Suárez,G. (1994). An inverted double seismic zone in Chile: evidence of phase transformation in the subducted slab. Science, 263, 212-215.
[12] Comte,D., Roecher,S.W., Suárez,G. (1994). Velocity structure in northern Chile: evidence of subducted oceanic crust in the Nazca plate. Geophys. J.Int. 117, 625-639.
[13] Daniel,J.W. (1971). The Approximate Minimization of Functionals, Publishers Englewood Cliff, NJ.
[14] Delouis,B., Cisternas,A., Dorbath,L., Ribera,L., Kausel,E. (1996). The Andean subduction zone between 22 and 25°S (northern Chile): precise geometry and state of stress. Tectonophysics, 259, 81-100.
[15] Dewey,J.F, Lamb,S.H.(1992). Active tectonics of the Andes. Tectonophysics, vol.205,79-95.
[16] Engdahl, E.R., Van der Hilst, R.D., Berrocal,J. (1995). Imaging of subducted lithosphere beneath South America. Geophys.Ress.Lett. 22,2317-2320.
[17] Giese et a. (1998). Journal of South American Earth Sciences 12 (1999),201-220.
[18] Grange,F., Rodrigues,A., Ocola,L. (1984). Tectonic implications of the microearthquakes seismicity and fault plane solutions in southern Peru and their implications. J. Geophys. Res. 89, 6139-6152.
[19] Hasegawa,A. Sacks,I.S. (1981). Subduction of the Nazca plate beneath Peru as determined from seismic information. J.Geophys. Res.,86, 4971-4980.
[20] Haslinger,J., Hlaváček,I., Nečas,J. (1996). Numerical Methods for Unilateral Problems in Solid Mechanics. In: Handbook of Numerical Analysis. Vol.IV, 313-486, Elsevier Science, Amsterdam.
[21] Hlaváček, I., Haslinger, J., Nečas, J., Lovíšek, J. (1988). Solution of Variational Inequalities in Mechanics. Springer Vlg., New York.
[22] Isacks,B.L., Molnar,P. (1971). Distribution of stress in the descending lithosphere from a global survey of focal mechanism solution of mantle earthquakes. Rev. Geopys. Space Phys., 9,103-174.
[23] Jarušek,J. (1983). Contact problems with bounded friction: coercive case, Czech Math.J., 33,2, 237-261.
[24] Jordan,T.E., Isacks, B.L., Allmendinger, R.W., Brewer, J.A., Ramas,V.A., Ando,C.J. (1983). Andean tectonics related to geometry of subducted Nazca Plate. Geol.Soc.Am. Bull. 94,341-361.
[25] Lopèz-Escobar,L., Cembrano,J., Moreno,H. (1995). Geochemistry and tectonics of the Chilean Southern Andes basaltic Quarternary volcanism (37-46°S). Revista Geologica De Chile, vol. 22, no 2, 219-234.
[26] Luenberger, D.G. (1984). Linear and Non-linear Programming, Addison-Wesley Publishing Company, Reading, Massachussetts, Menlo Park, California, London, Amsterdam, Ontario, Sydney.
[27] Muñoz,J.B, Stern,C.R. (1988). The Quarternary volcanic belt of the southern continental margin of South America: Transverse structural and petrochemical variations across the segment between 38°S and 39°S. Jornal of South American Earth Sciences. vol. 1,No.2, 147-161.
[28] Nedoma,J. (1982). Thermo-elastic stress-strain analysis of the geodynamic mechanism. Gerlands Beitr. Geophysik, 91,1,75-89.
[29] Nedoma, J. (1983). One one type os Signorini problem without friction in linear thermo-elasticity: the quasi-coupled 2D-case. Appl. Math., 28,6,393-407.
[30] Nedoma,J. (1986a-c). On the geodynamic model of the Earth and the plate tectonic hypothesis. I-III. Gerlands Beitr. Geophysik, 95,1,36-62, 95,2,89-105.
[31] Nedoma,J. (1987). On the Signorini problem with friction in linear thermo-elasticity: the quasi-coupled 2D-case. Appl.Math. 32,3, 186-199.
[32] Nedoma,J. (1990a). Tectonic evolution of collision zones, I. Mechanics of tectonic processes. II. Subducted lithosphere. Gerlands Beitr.Geophysics (I) 99,2,97-108, (II) 99,2,109-121.
[33] Nedoma,J. (1990b). On a new theory of earthquke mechanism. In: Proc. 4th Int. Symp. on Analysis of Seismicity and Seismic Risk (Schenkova, Z., Ed.) Geophys.Inst. Czech.Acad.Sci, Prague, 339-346.
[34] Nedoma,J. (1990c). Plate tectonics and the analysis of fracture mechanics in a collision zone, I,II. Contr. Geophys. Inst. Slov. Acad.Sci, 20,53-69, 21,38-58.
[35] Nedoma,J. (1994). Finite element analysis of contact problems in thermo-elasticity: the semi-coercive case. J.Comput. Appl.Math., 50,411-423.

[36] Nedoma,J. (1998). Numerical Modelling in Applied Geodynamics. John Wiley&Sons, Chichester, New York, Weinheim, Brisbane, Singapore, Toronto.
[37] Nedoma,J., Bartoš,M.,Kestřánek,Z., Kestřánek,Z.jr., Stehlík,J. (1999). Numerical methods for optimization in 2D and 3D biomechanics. Numerical Linear Algebra Appl. 6,567-586.
[38] Nedoma, J. (2000). Dynamic contact problems with friction in elasticity and thermo-elasticity. Proc. of the 4th conference on Numerical Modelling in Continuum Mechanics. Theory, algorithms, applications. Prague, July 31-August 3,2000 (in print).
[39] Rodrigues,L., Tavera,J. (1991). Determinación con alta resolución dela geometria dela zona Wadati-Benioff en el Peru central. Rev.Bras. Geof. (submitted)
[40] Sacks, I.S. (1977). Interrelationships between volcanism, seismicity and inelasticity in western South America. Tectonophysics, 37, 131-139.
[41] Schenker,E., Giese,P. (1999). Journal of South American Earth Sciences 12(1999), 103-107.
[42] Smalley,R.F.,Isacks,B.L.(1987). A high-resolution local network of the Nazca plate Wadati-Benioff zone under western Argentina. J.Geophys.Res. 92;13903-13912.

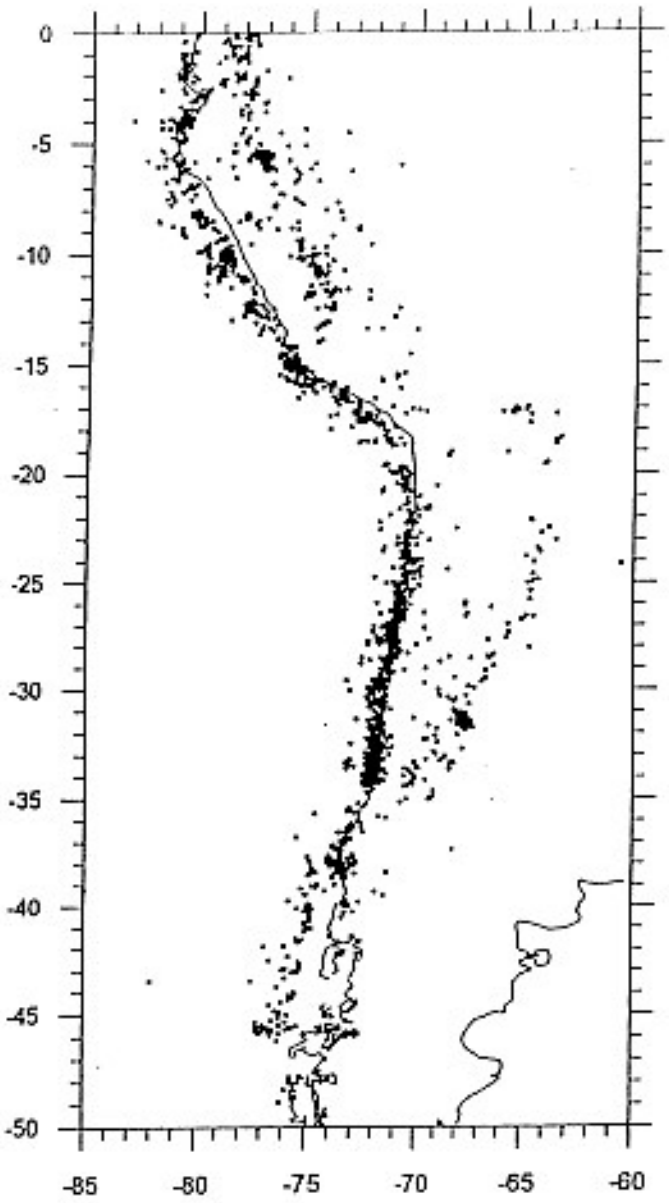


Fig.1a

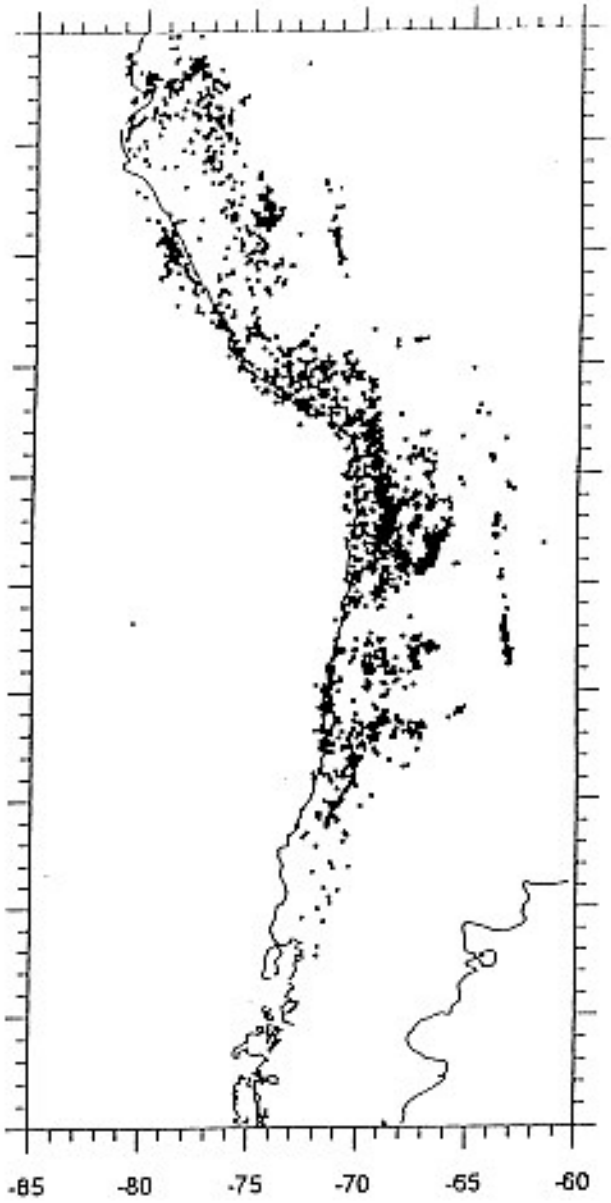


Fig.1b

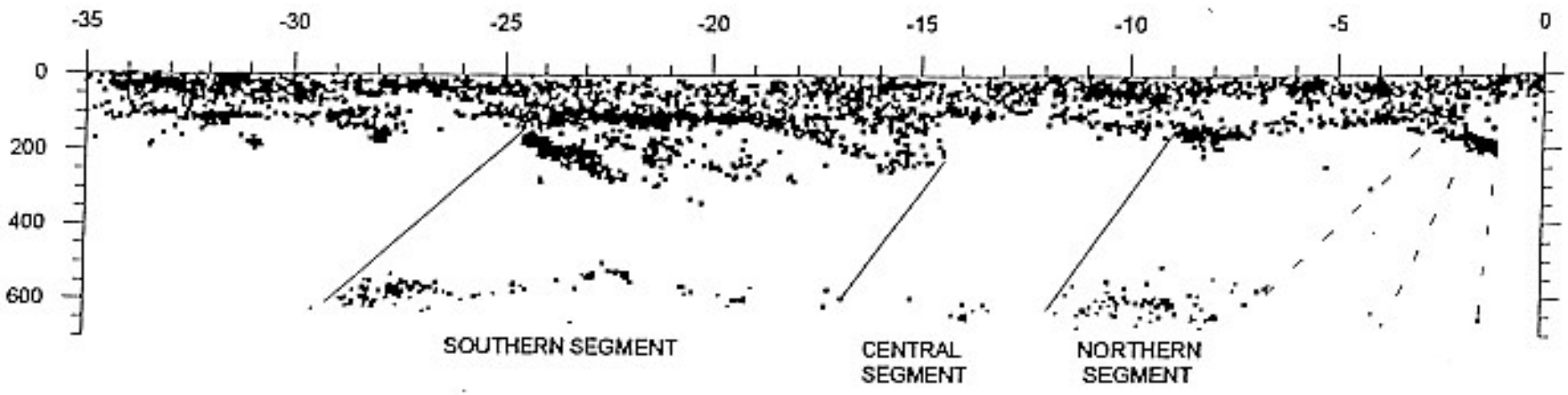
-35
-30
-25
-20
-15
-10
-5
0
0
200
400
600
SOUTHERN SEGMENT
CENTRAL
SEGMENT
NORTHERN
SEGMENT

Fig.1c

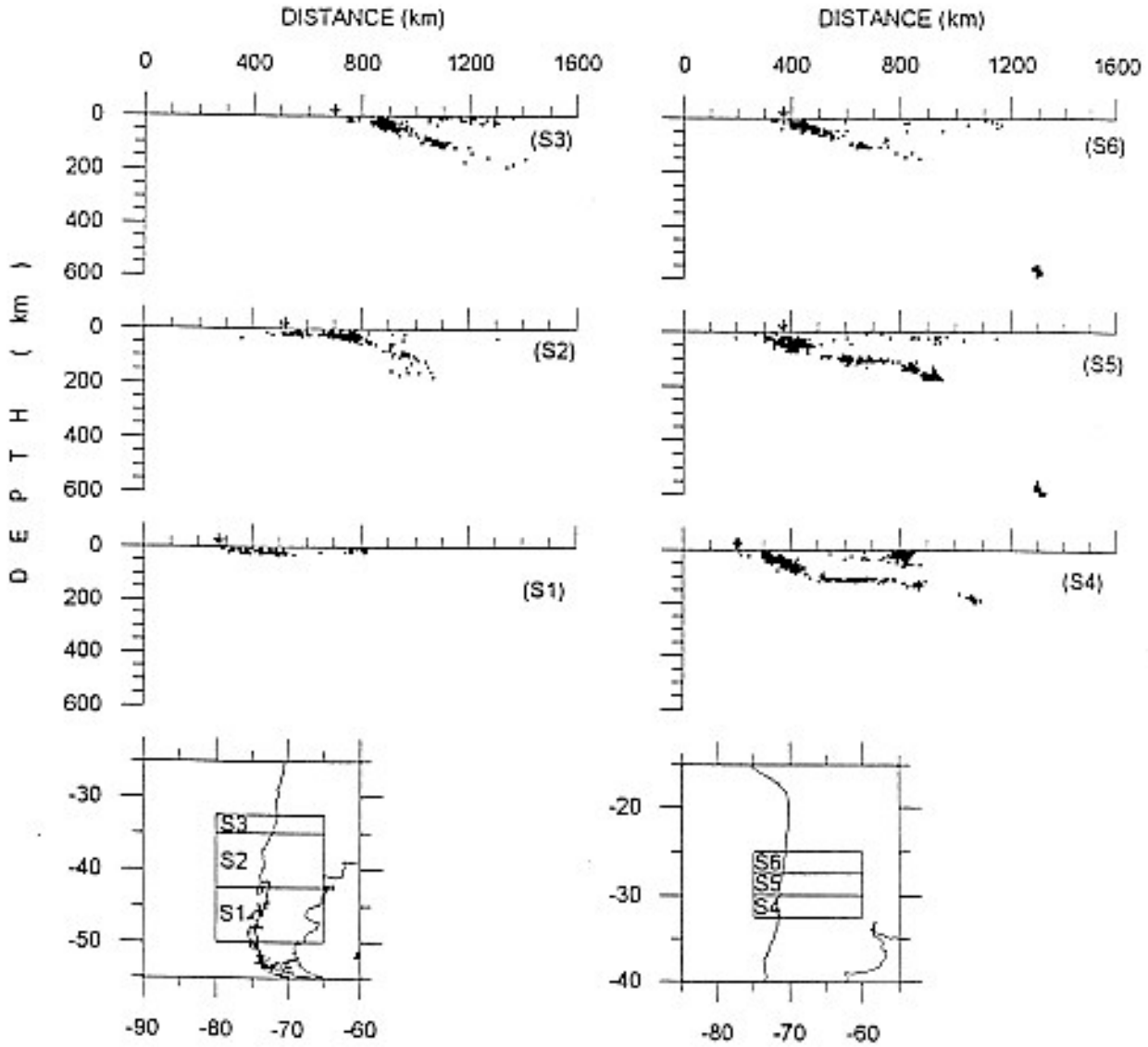
DISTANCE (km)
0
400
800
1200
1600
DEPTH ( km )
0
200
400
600
(S3)
(S2)
(S1)
DISTANCE (km)
(S6)
(S5)
(S4)
-30
-40
-50
-90
-80
-70
-60
S3
S2
S1
-20
-30
-40
S6
S5
S4

Figs 2a-f

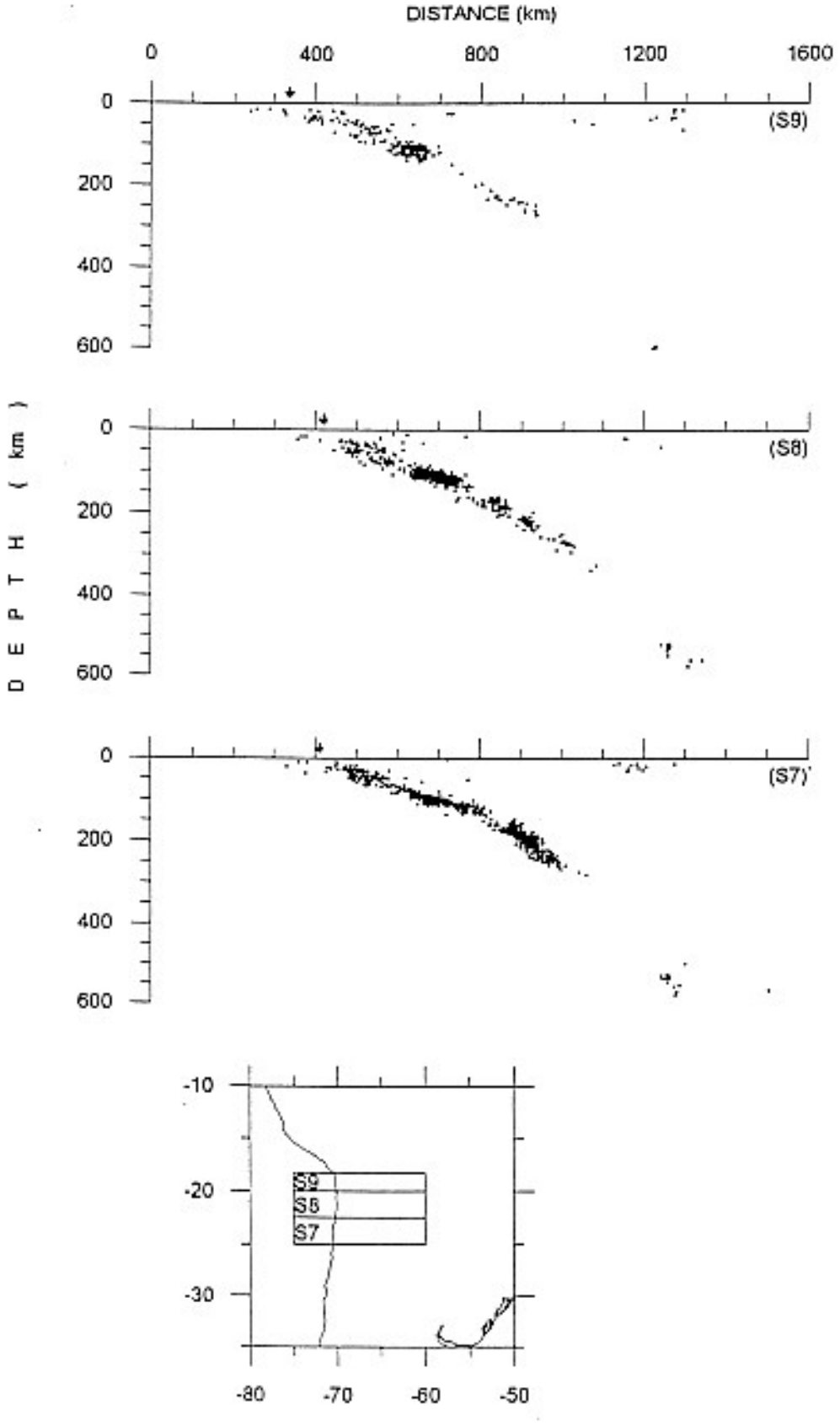
DISTANCE (km)
0
400
800
1200
1600
DEPTH (km)
0
200
400
600
(S9)
(S8)
(S7)
-10
-20
-30
-80
-70
-60
-50
S9
S8
S7

Figs 2g-i

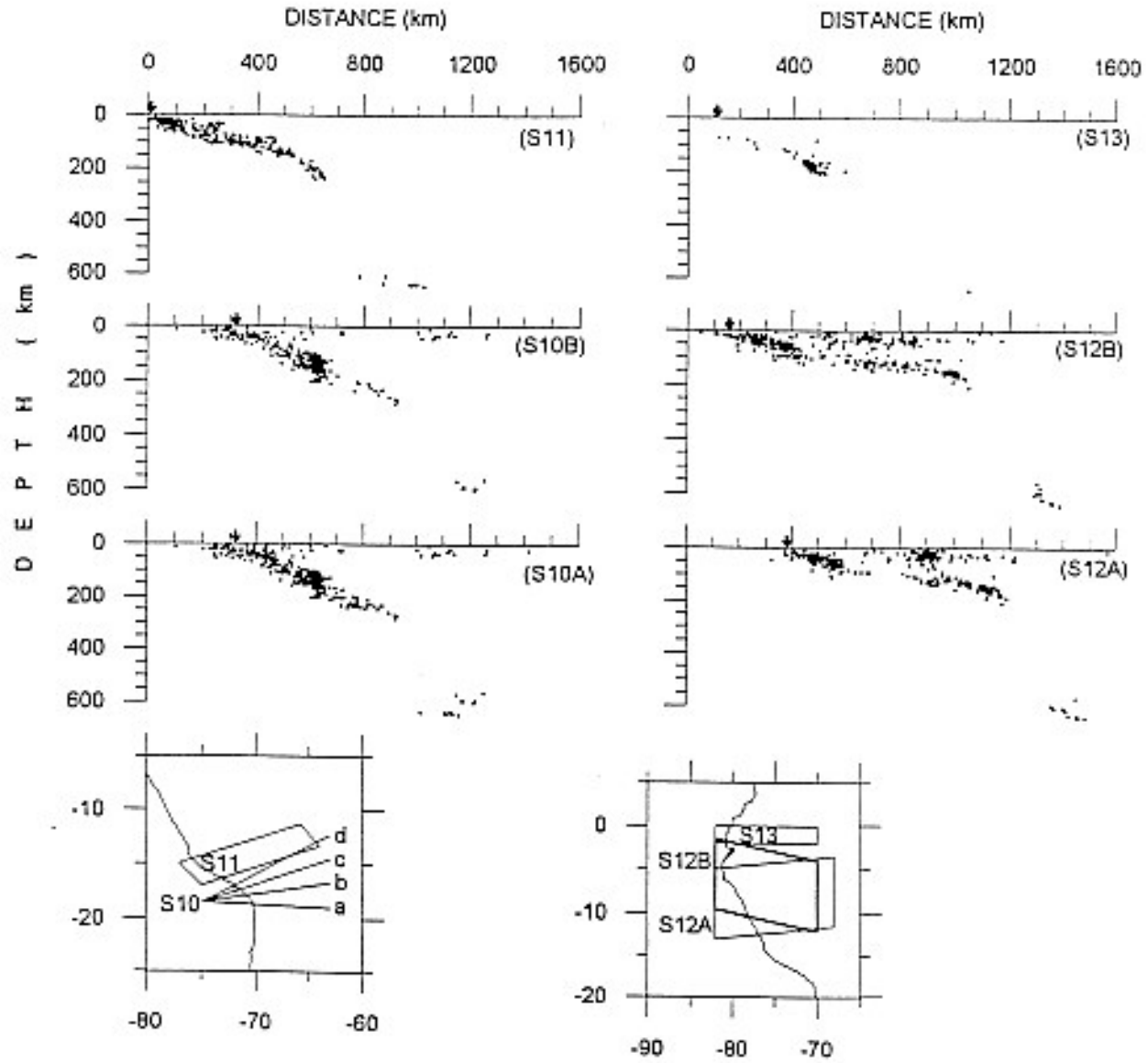
DISTANCE (km)
0
400
800
1200
1600
DEPTH (km)
0
200
400
600
(S11)
(S10B)
(S10A)
DISTANCE (km)
(S13)
(S12B)
(S12A)
-10
-20
S11
S10
d
c
b
a
-80
-70
-60
0
S13
S12B
S12A
-90
-80
-70

Figs 2j-o

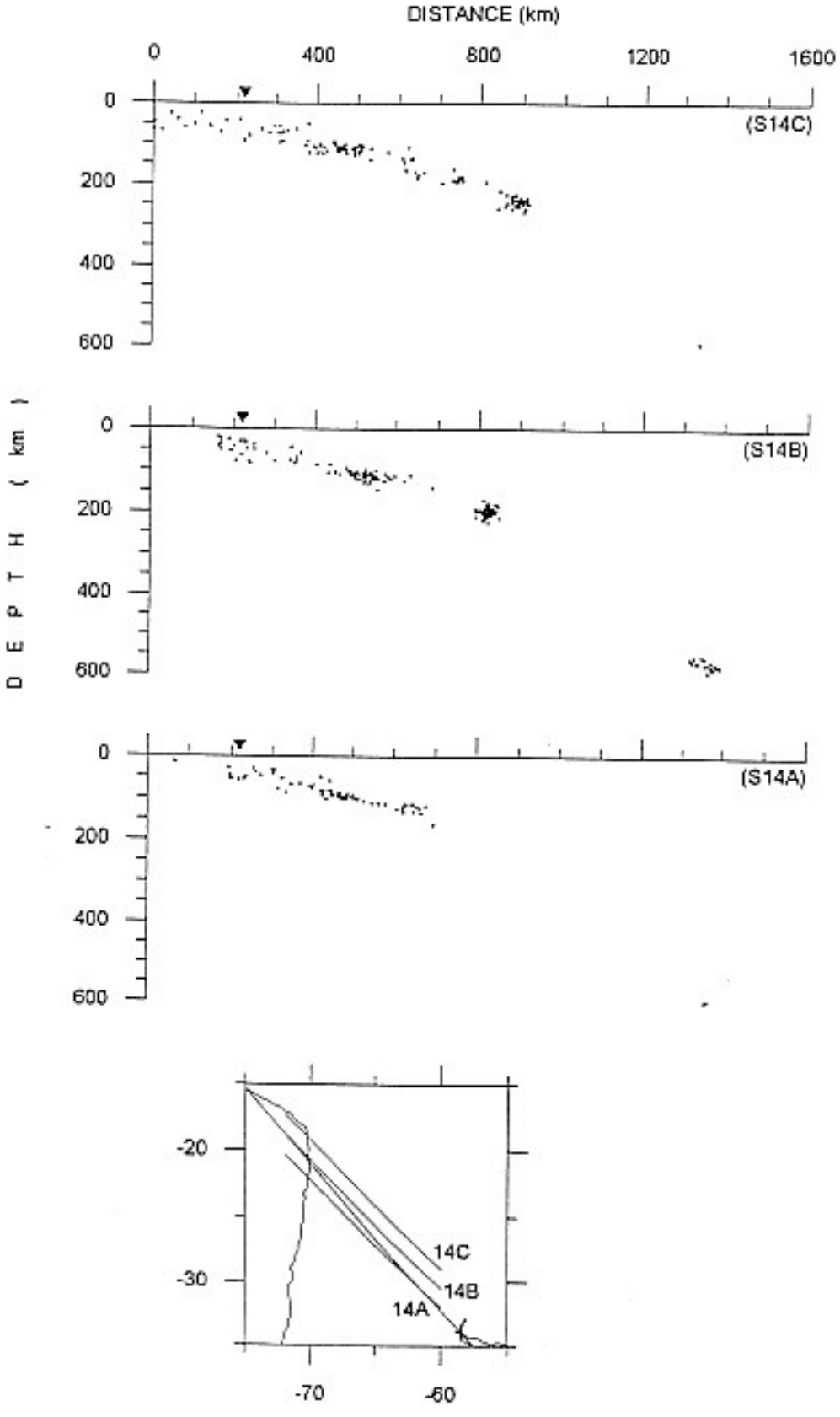
DISTANCE (km)
0
400
800
1200
1600
0
200
400
600
(S14C)
(S14B)
(S14A)
D E P T H ( km )
-20
-30
-70
-60
14C
14B
14A

Figs 2p-r

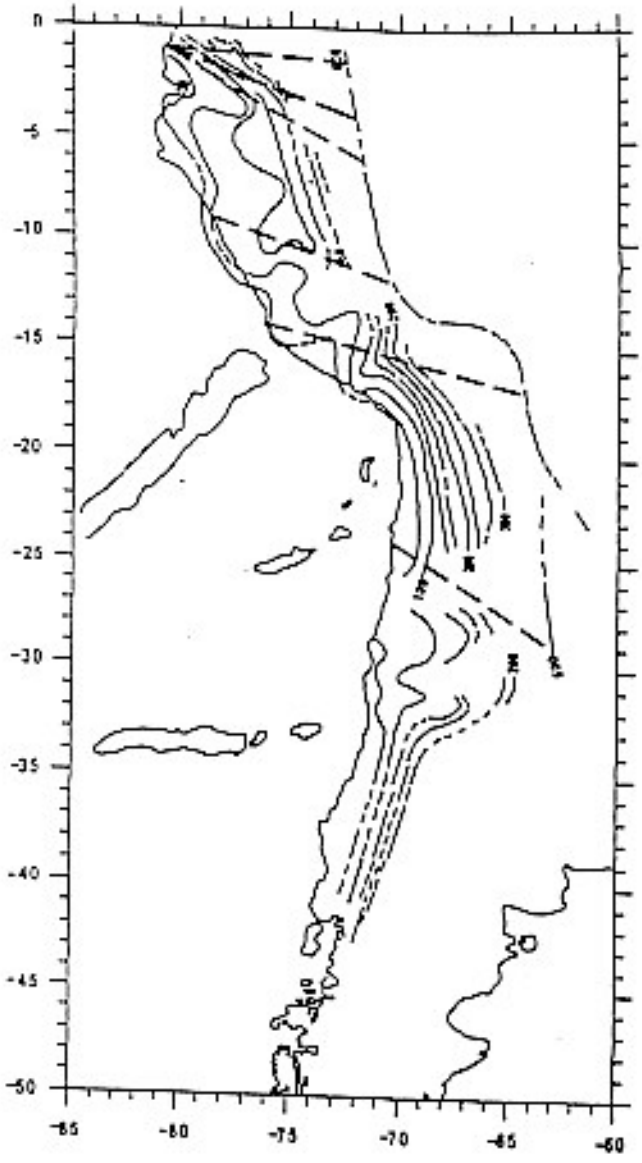


Fig.3

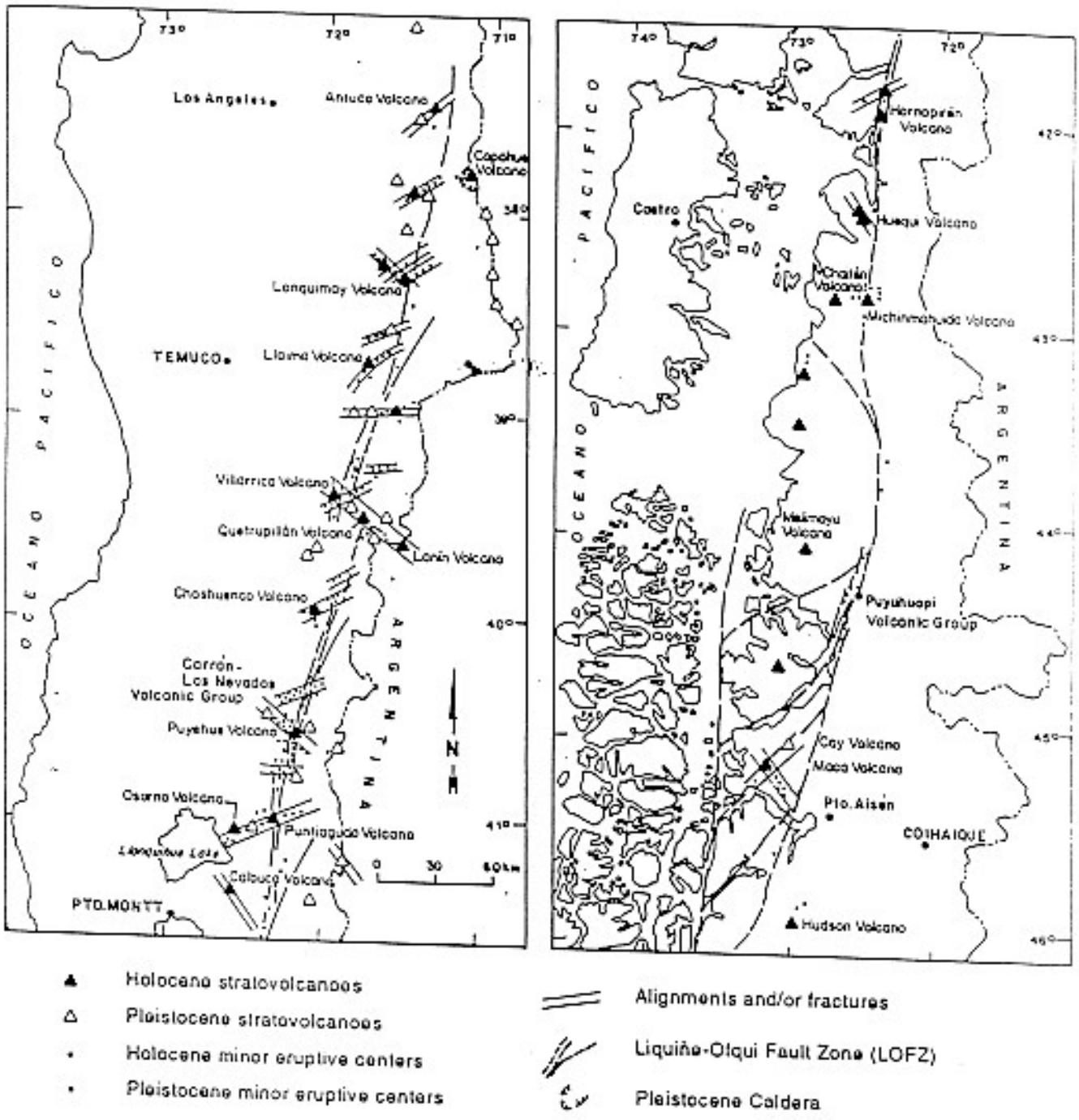
Los Angeles
Antuco Volcano
Copahue Volcano
Lonquimay Volcano
TEMUCO
Llaima Volcano
Villarrica Volcano
Quetrupillán Volcano
Lanín Volcano
Choshuenco Volcano
Carrán-
Los Nevados
Volcanic Group
Puyehue Volcano
Osorno Volcano
Punta Agudo Volcano
Calbuco Volcano
PTO. MONTT
OCEANO PACIFICO
ARGENTINA
N
0 30 60 km
Hernopirén Volcano
Castro
Hueque Volcano
Chaitén Volcano
Michinmahuida Volcano
Melimoyu Volcano
Puyuhuapi
Volcanic Group
Cay Volcano
Maca Volcano
Pto. Aisén
COIHAIQUE
Hudson Volcano
Holocene stratovolcanoes
Pleistocene stratovolcanoes
Holocene minor eruptive centers
Pleistocene minor eruptive centers
Alignments and/or fractures
Liquiñe-Ofqui Fault Zone (LOFZ)
Pleistocene Caldera

Fig.4a

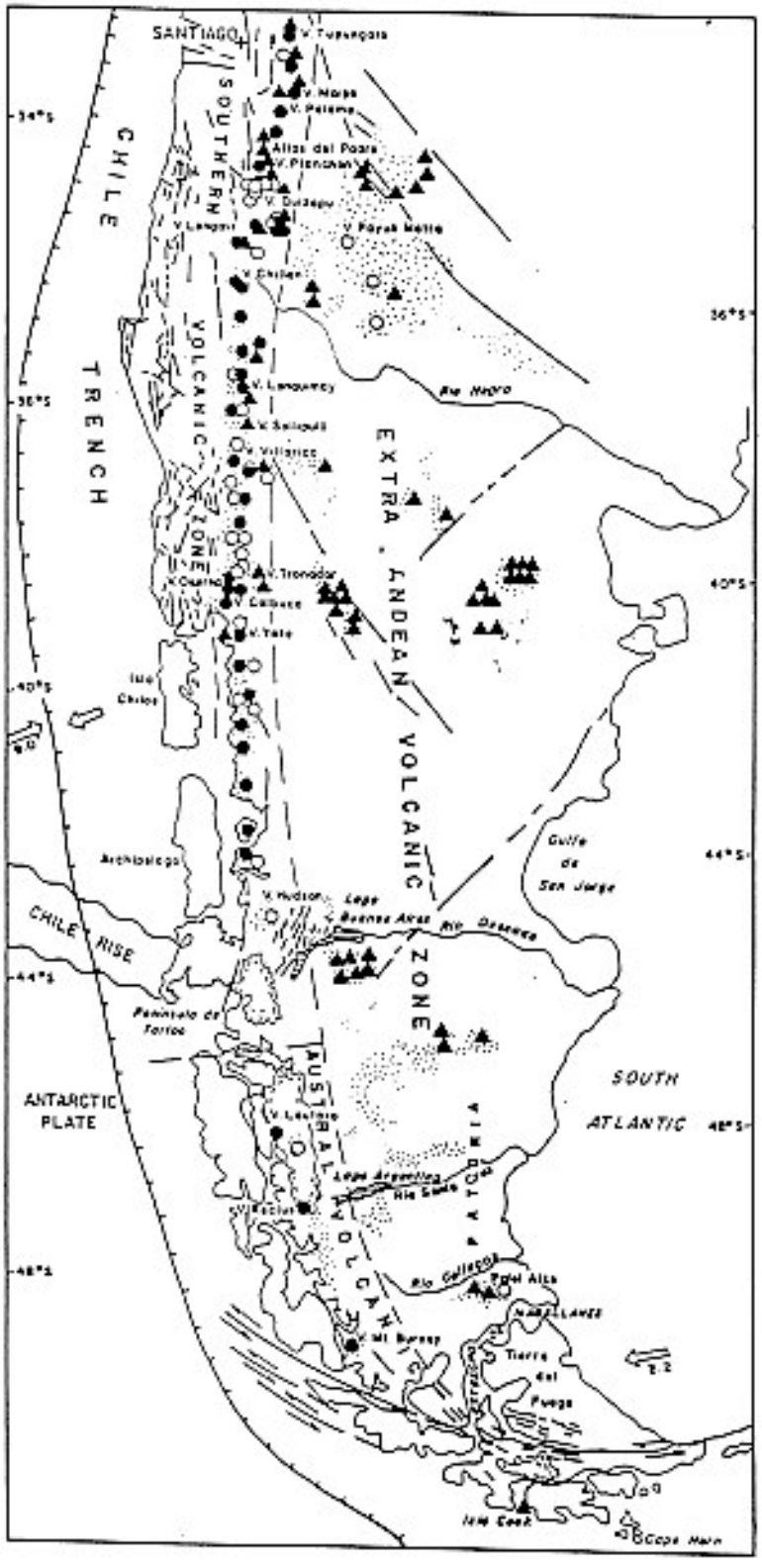
SANTIAGO
CHILE TRENCH
SOUTHERN VOLCANIC ZONE
EXTRA - ANDEAN VOLCANIC ZONE
AUSTRAL VOLCANIC ZONE
CHILE RISE
ANTARCTIC PLATE
SOUTH ATLANTIC
34°S
36°S
38°S
40°S
42°S
44°S
46°S
48°S
Río Negro
Archipiélago de Chiloé
Golfo de San Jorge
Lago Buenos Aires
Río Deseado
Península de Taitao
Lago Argentino
Río Santa Cruz
Río Gallegos
Monte Aymond
Tierra del Fuego
Estrecho de Magallanes
Isla de los Estados
Cabo de Hornos

Fig.4b

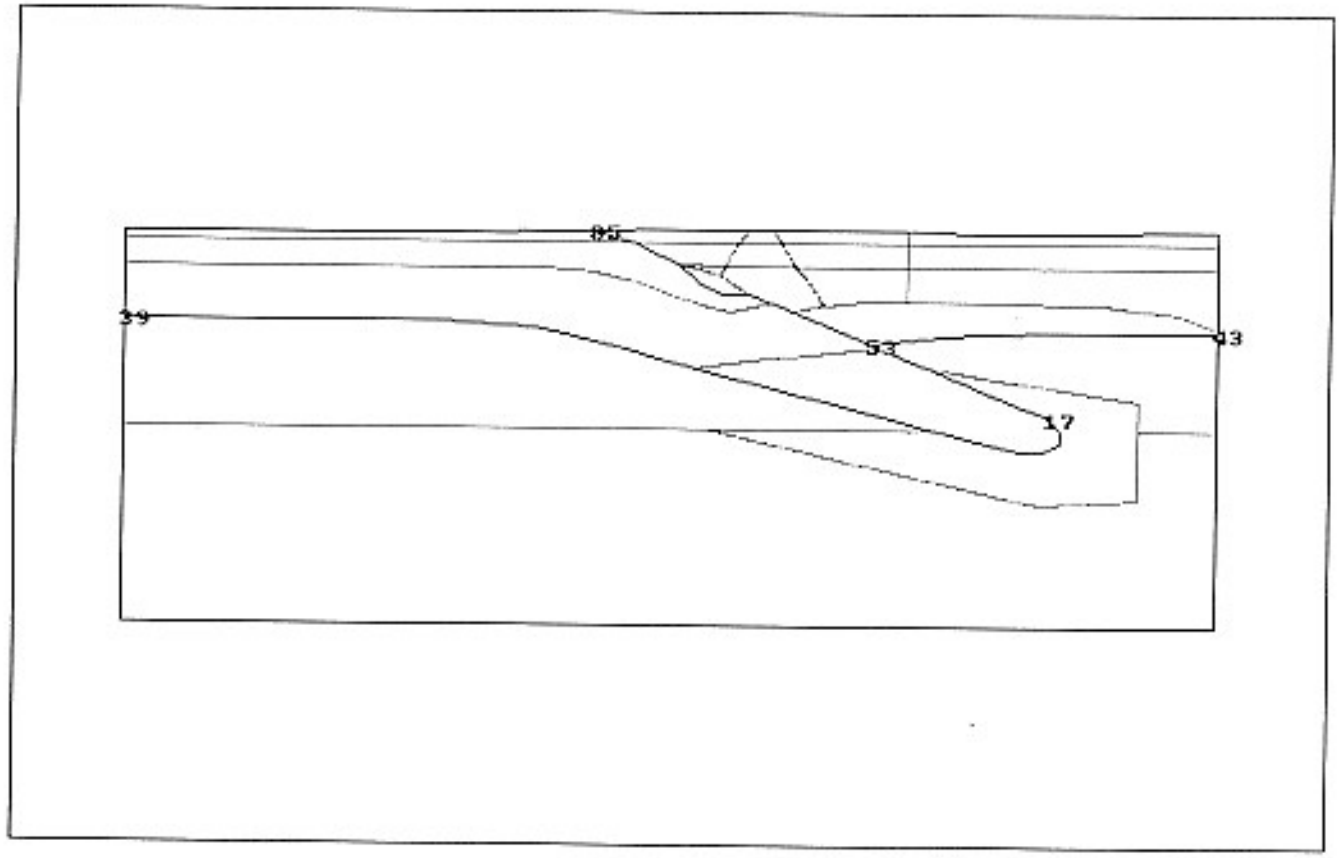


Fig.5

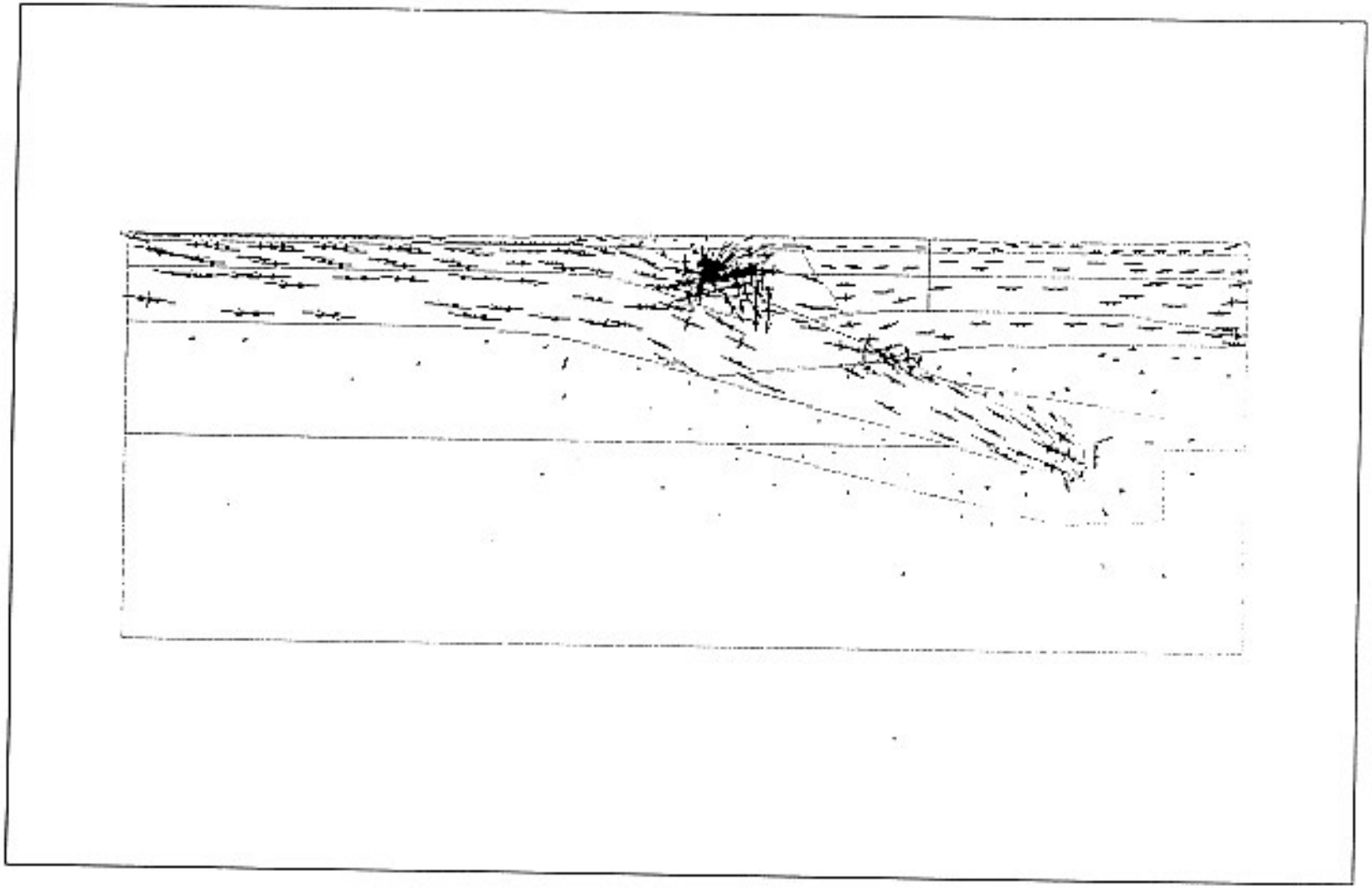

Fig.6a

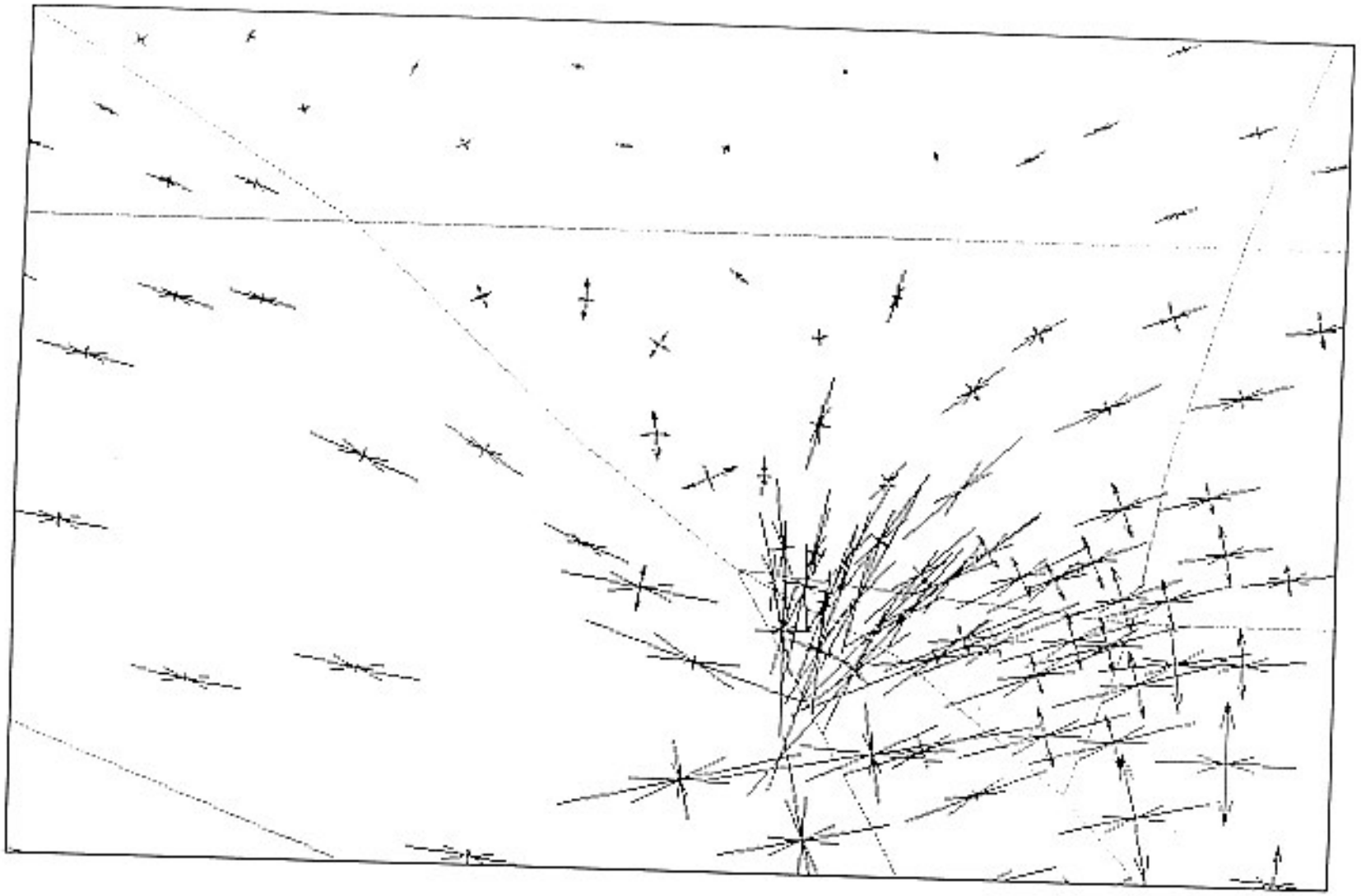

Fig.6b

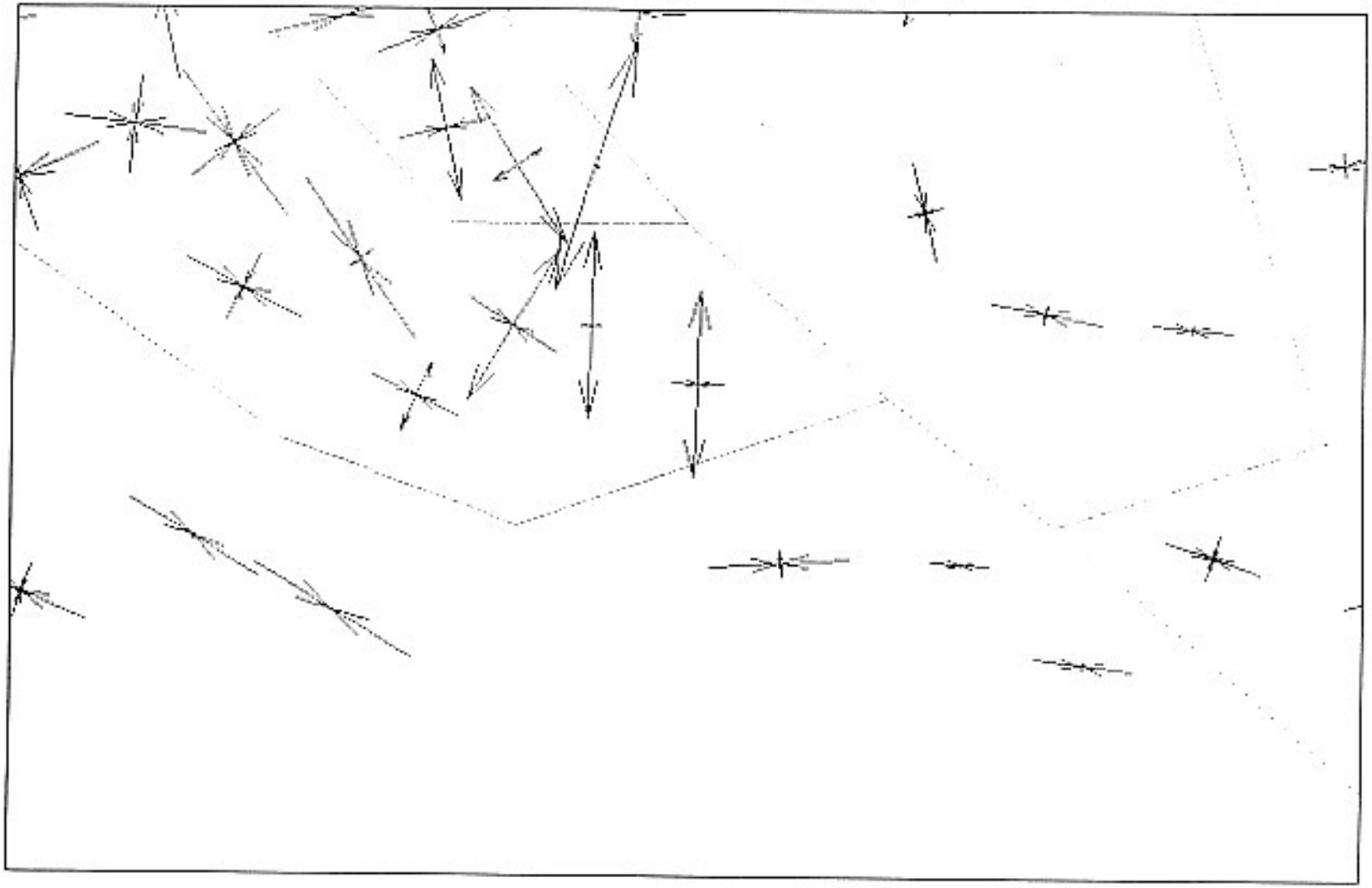

Fig.6c

p9 fig1

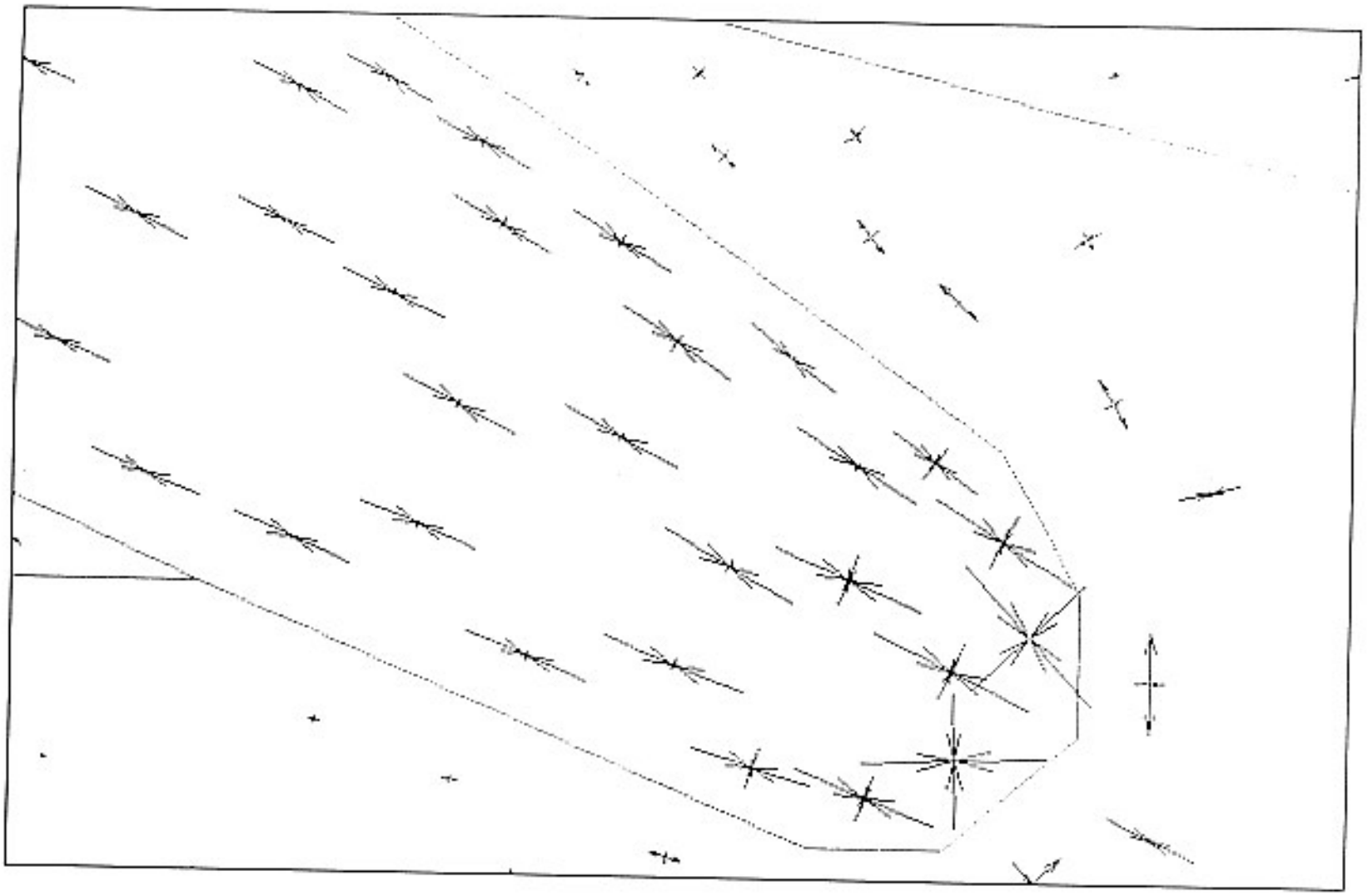

Fig.6e

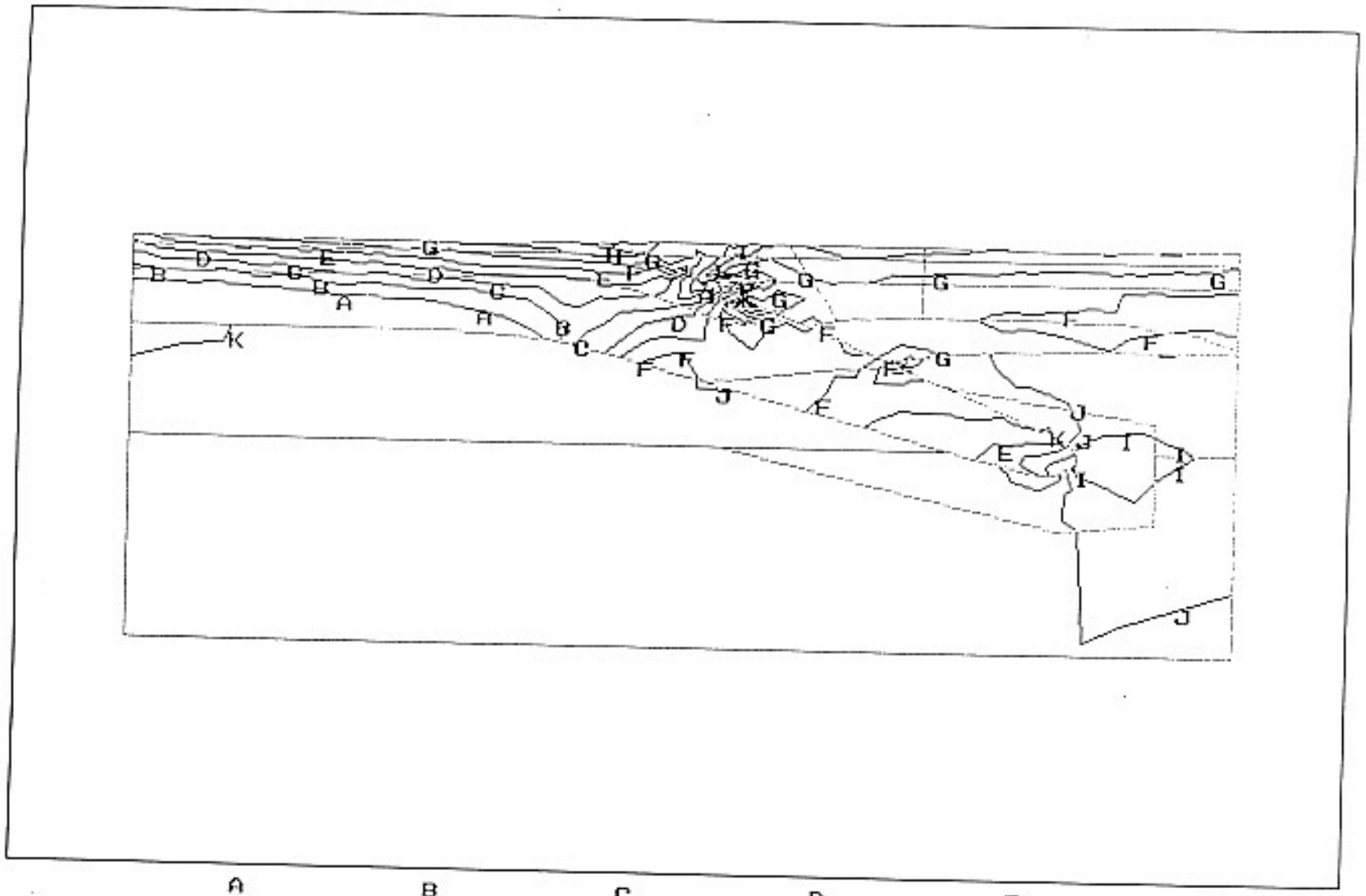

| | A | B | C | D | E | F |
|---|---|---|---|---|---|---|
| Sx | -3.551e+09 | -3.168e+09 | -2.785e+09 | -2.402e+09 | -2.019e+09 | -1.636e+09 |
| | G | H | I | J | K | L |
| | -1.253e+09 | -8.703e+08 | -4.873e+08 | -1.042e+08 | 2.788e+08 | 6.619e+08 |

Fig.6f

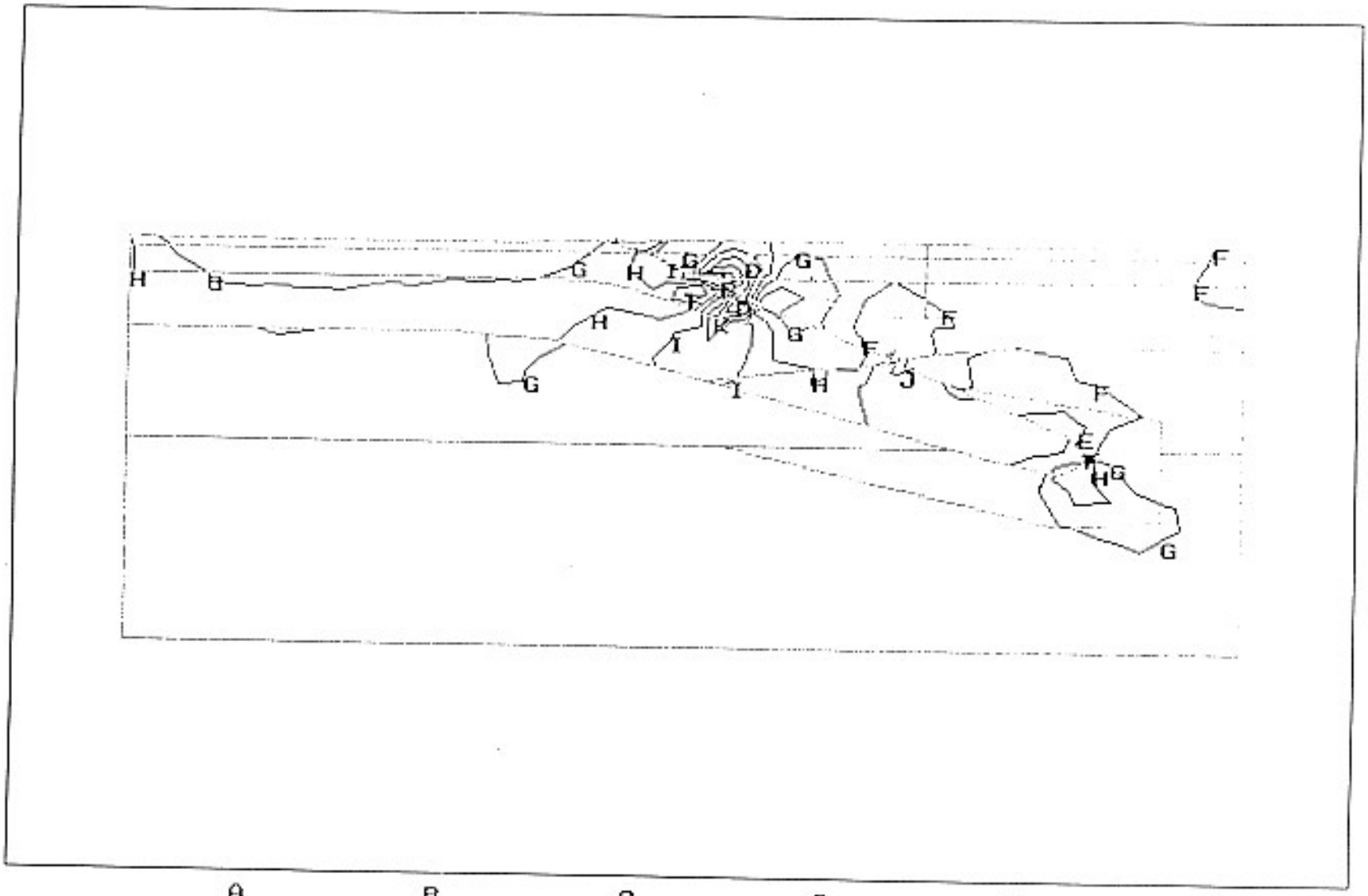

| | A | B | C | D | E | F |
|---|---|---|---|---|---|---|
| Sxz | -1.499e+09 | -1.223e+09 | -9.476e+08 | -6.719e+08 | -3.961e+08 | -1.203e+08 |
| | G | H | I | J | K | L |
| | 1.553e+08 | 4.311e+08 | 7.069e+08 | 9.826e+08 | 1.258e+09 | 1.534e+09 |

Fig.6g

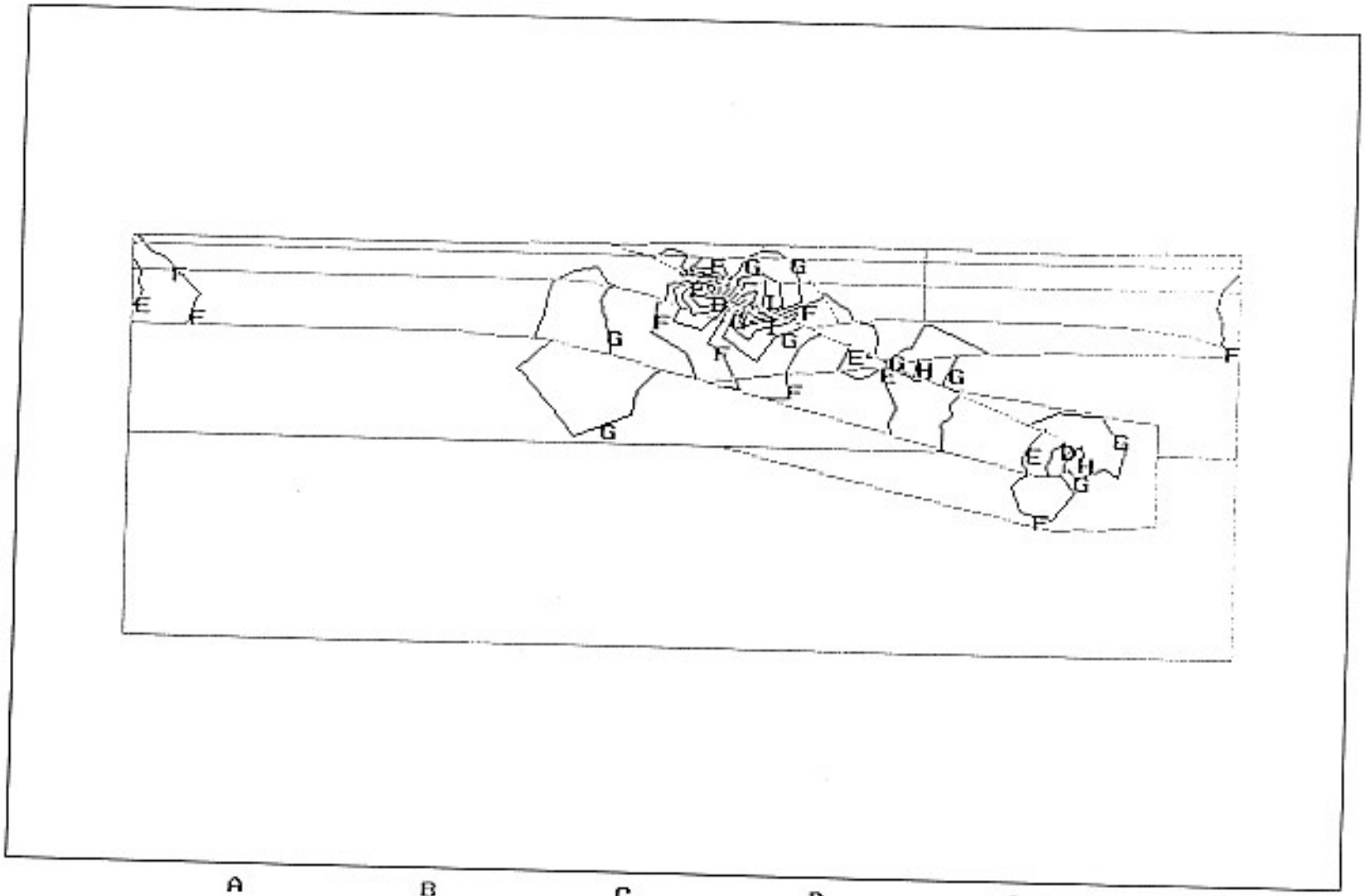

| | A | B | C | D | E | F |
|---|---|---|---|---|---|---|
| Sz | -3.138e+09 | -2.585e+09 | -2.032e+09 | -1.479e+09 | -9.266e+08 | -3.735e+08 |
| | G | H | I | J | K | L |
| | 1.795e+08 | 7.326e+08 | 1.285e+09 | 1.838e+09 | 2.391e+09 | 2.944e+09 |

Fig.6h

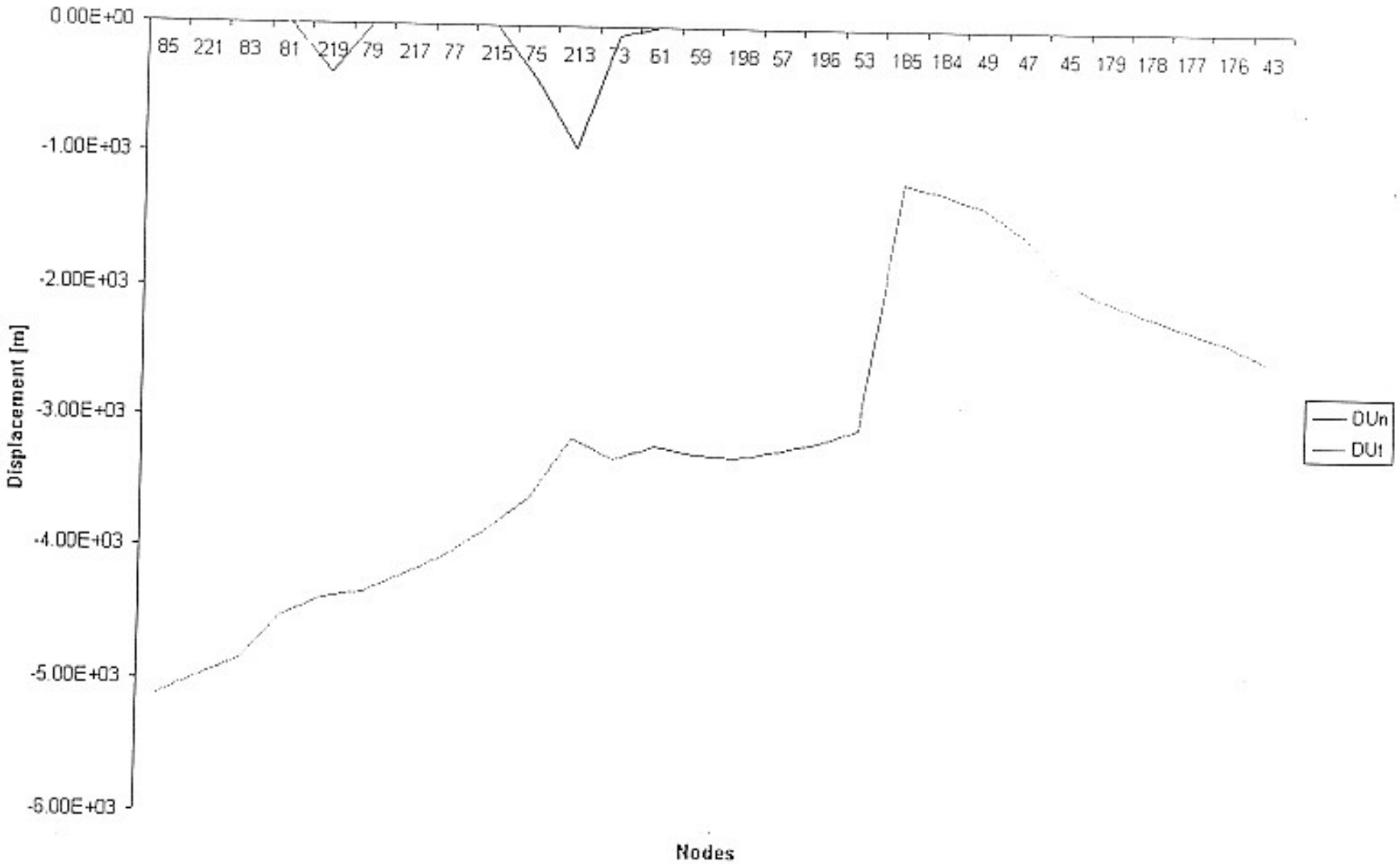
0.00E+00
-1.00E+03
-2.00E+03
-3.00E+03
-4.00E+03
-5.00E+03
-6.00E+03
Displacement [m]
85 221 83 81 219 79 217 77 215 75 213 73 61 59 198 57 196 53 185 184 49 47 45 179 178 177 176 43
Nodes
DUn
DU1

Fig. 7a

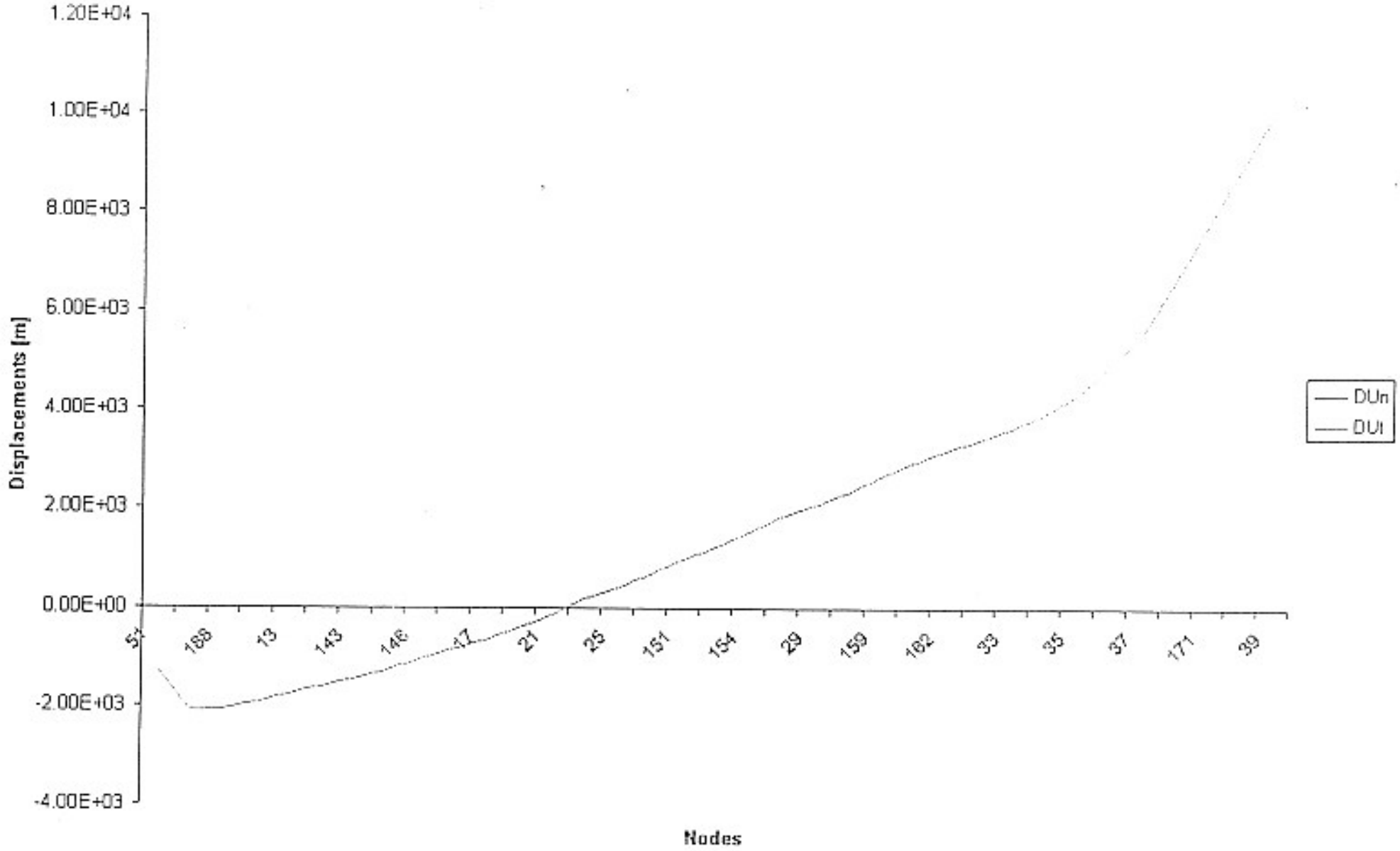
1.20E+04
1.00E+04
8.00E+03
6.00E+03
4.00E+03
2.00E+03
0.00E+00
-2.00E+03
-4.00E+03
Displacements [m]
51
168
13
143
146
17
21
25
151
154
29
159
162
33
35
37
171
39
Nodes
DUn
DUt

Fig.7b

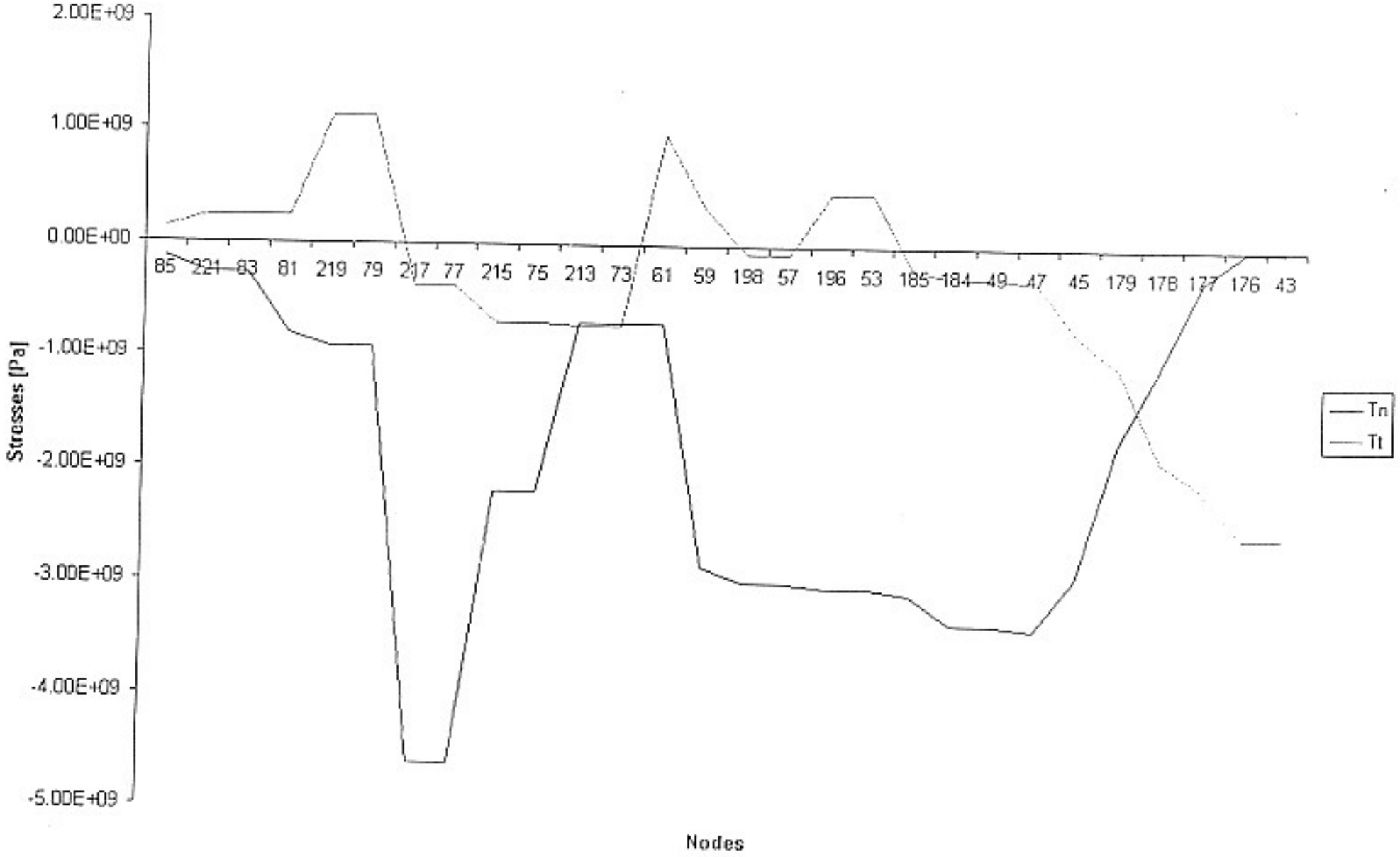
2.00E+09
1.00E+09
0.00E+00
-1.00E+09
-2.00E+09
-3.00E+09
-4.00E+09
-5.00E+09
Stresses [Pa]
85 221 83 81 219 79 217 77 215 75 213 73 61 59 198 57 196 53 185 184 49 47 45 179 178 177 176 43
Nodes
Tn
Tt

Fig.8a

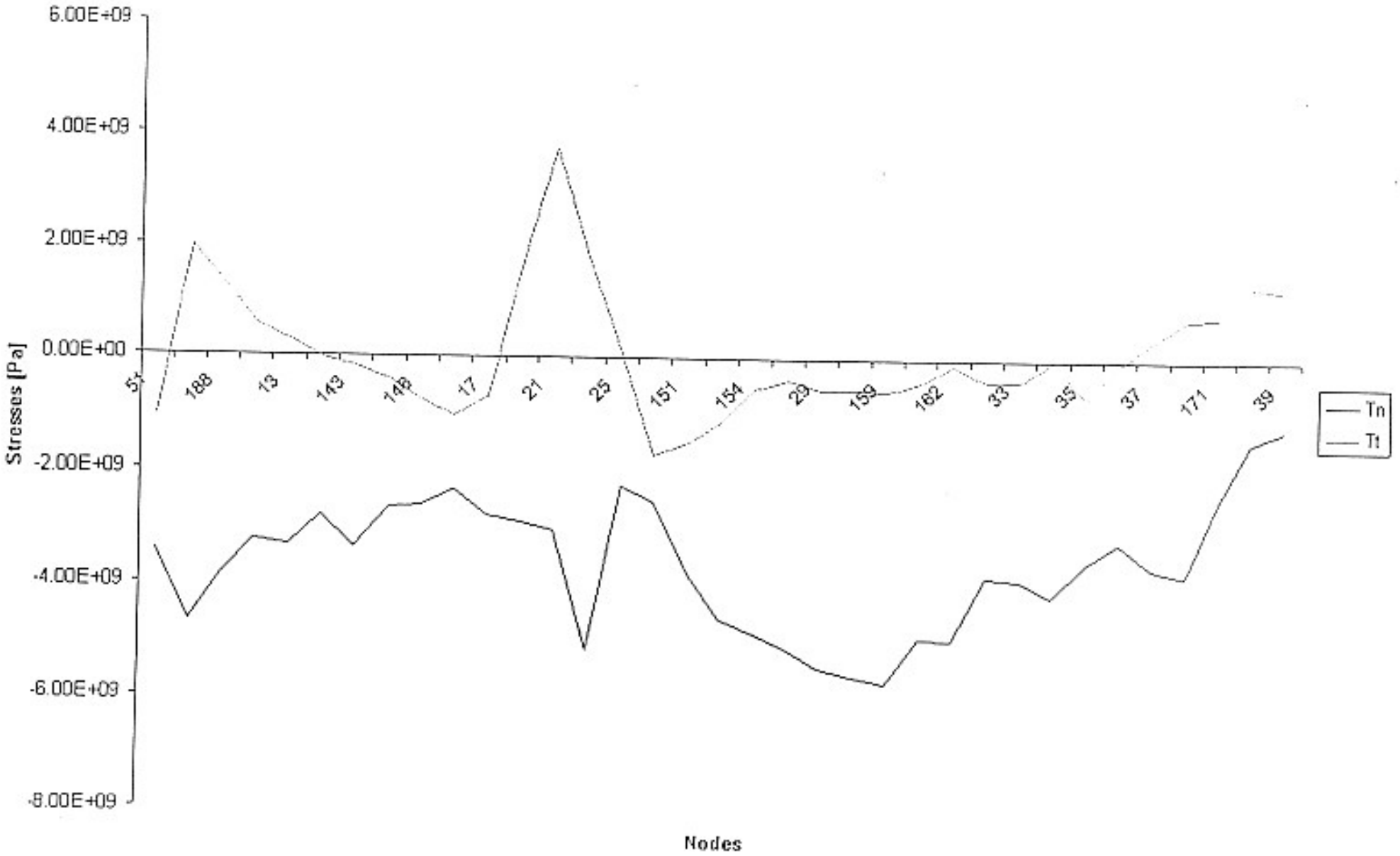
6.00E+09
4.00E+09
2.00E+09
0.00E+00
-2.00E+09
-4.00E+09
-6.00E+09
-8.00E+09
Stresses [Pa]
5
188
13
143
148
17
21
25
151
154
29
159
162
33
35
37
171
39
Nodes
Tn
Tt

Fig.8b

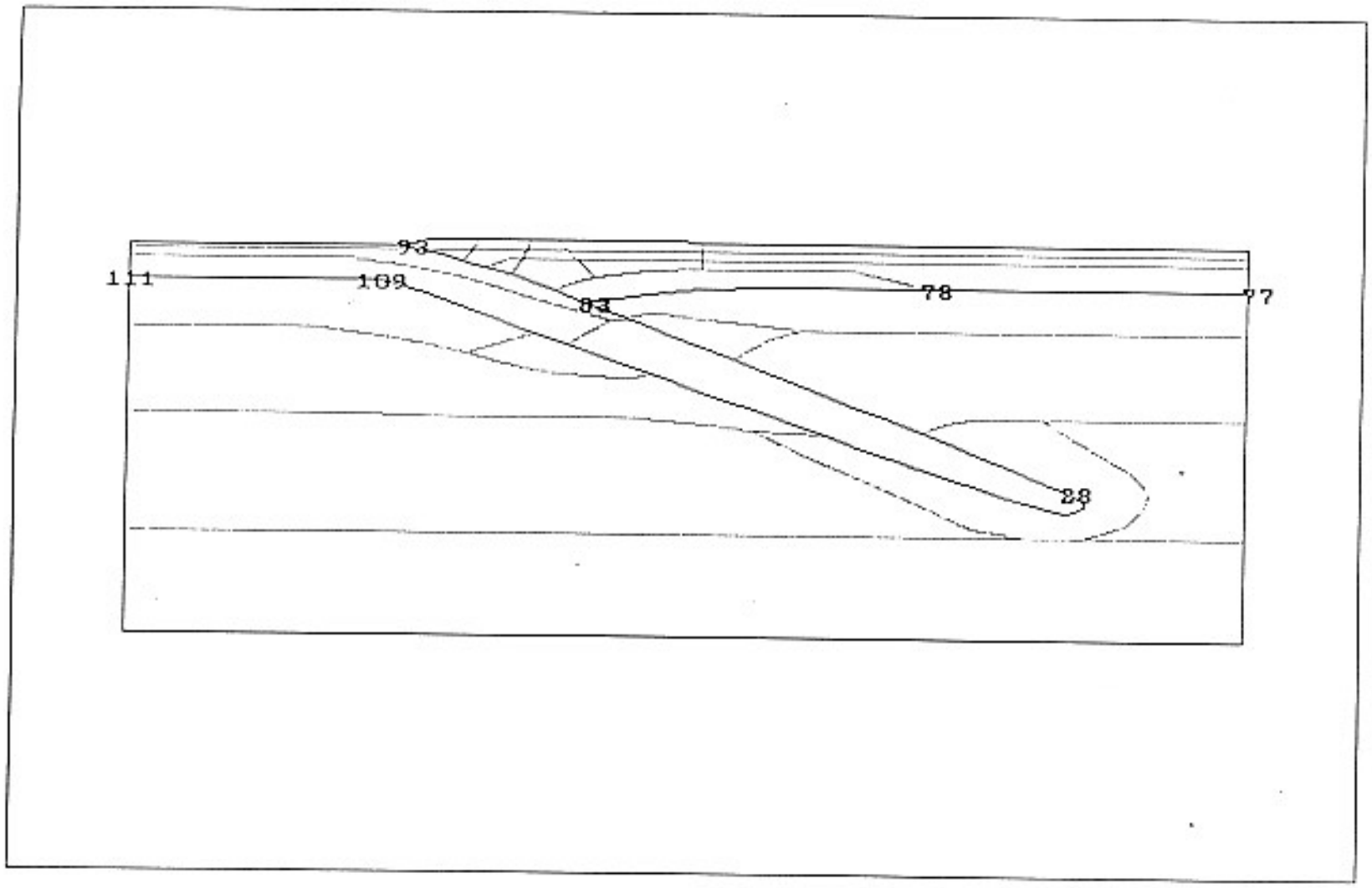


Fig.9

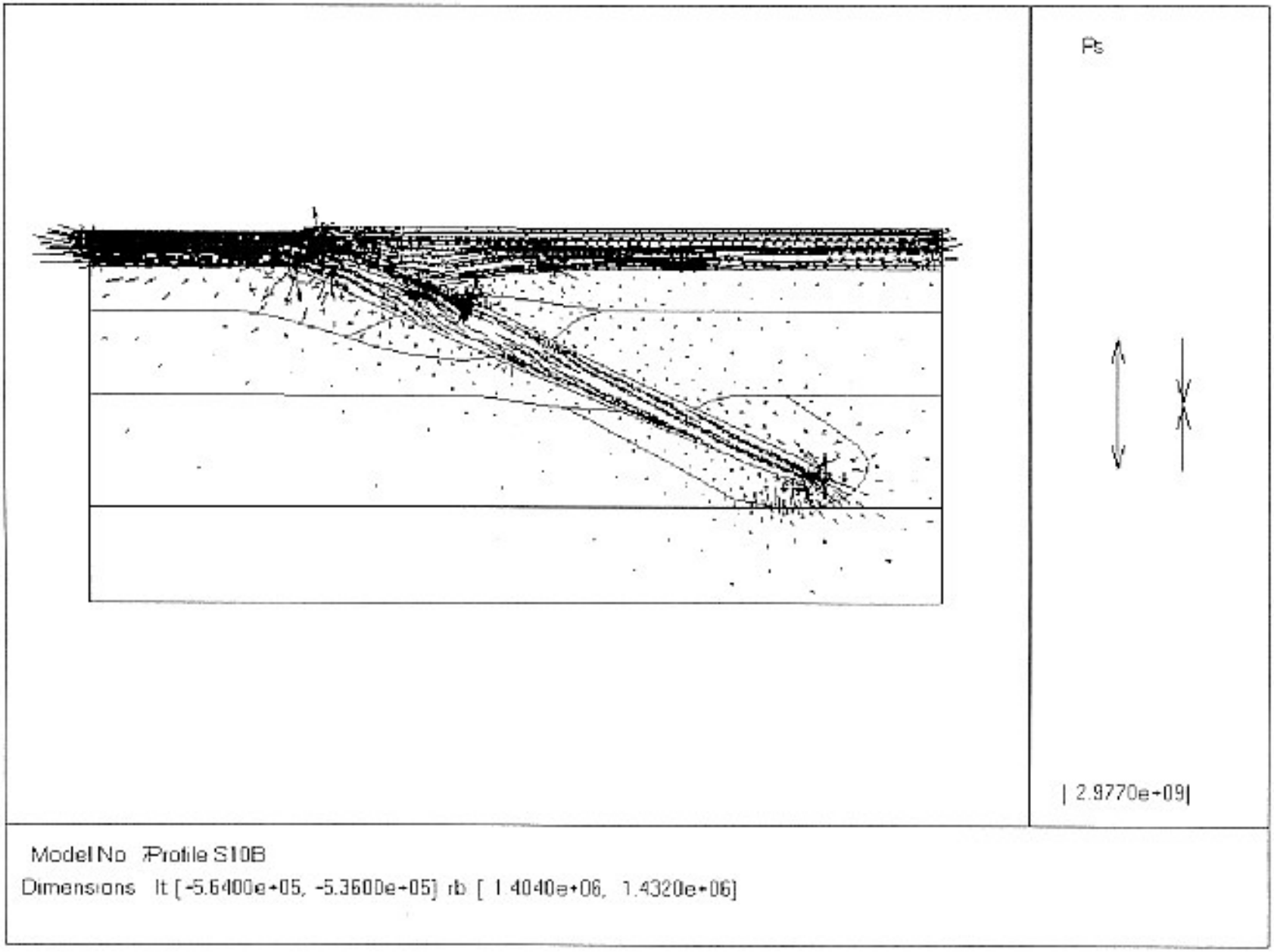
Ps
| 2.9770e+09|
Model No /Profile S10B
Dimensions lt [-5.6400e+05, -5.3600e+05] rb [ 1.4040e+06, 1.4320e+06]

Fig.10a

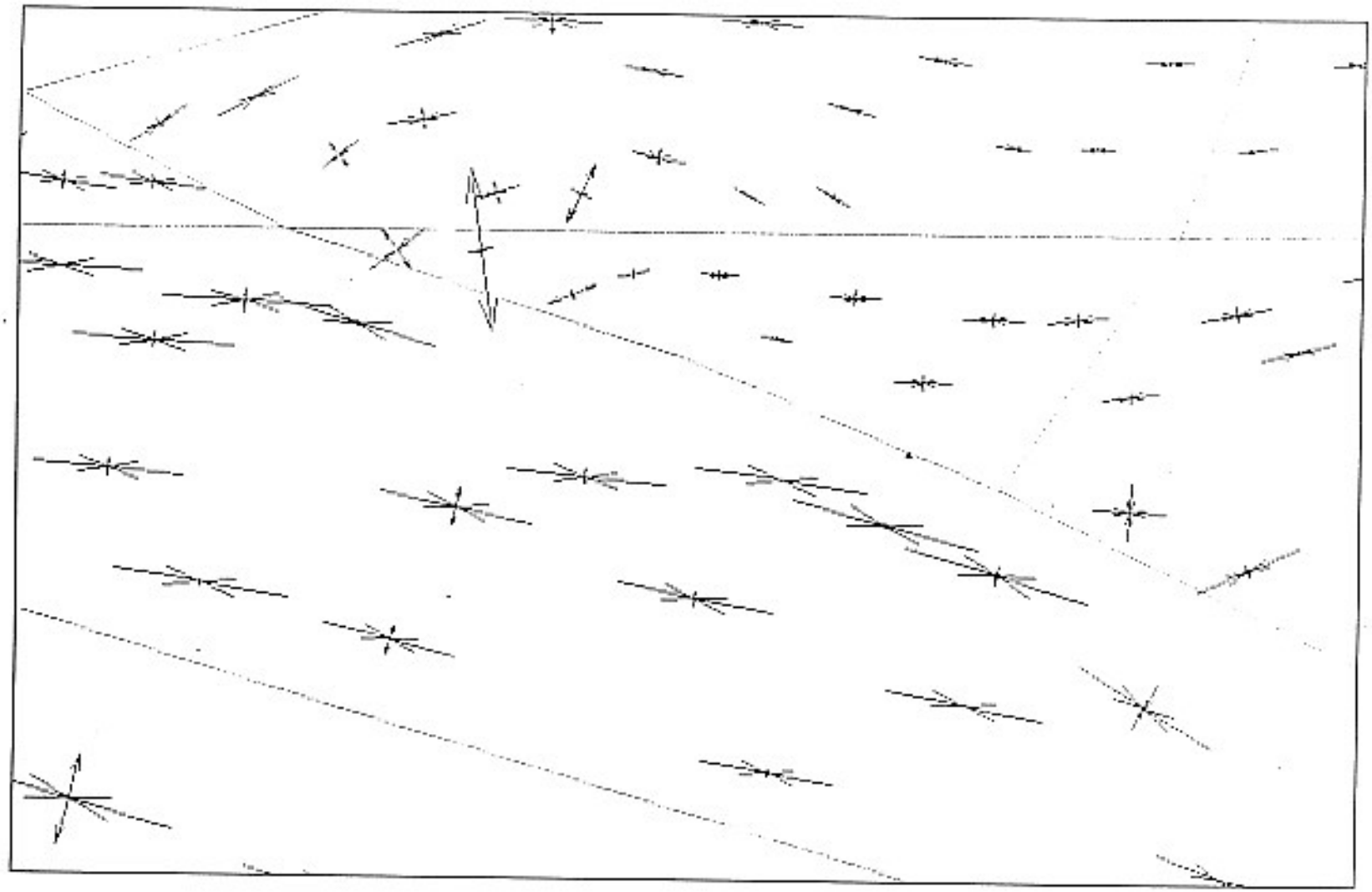

Fig. 10b

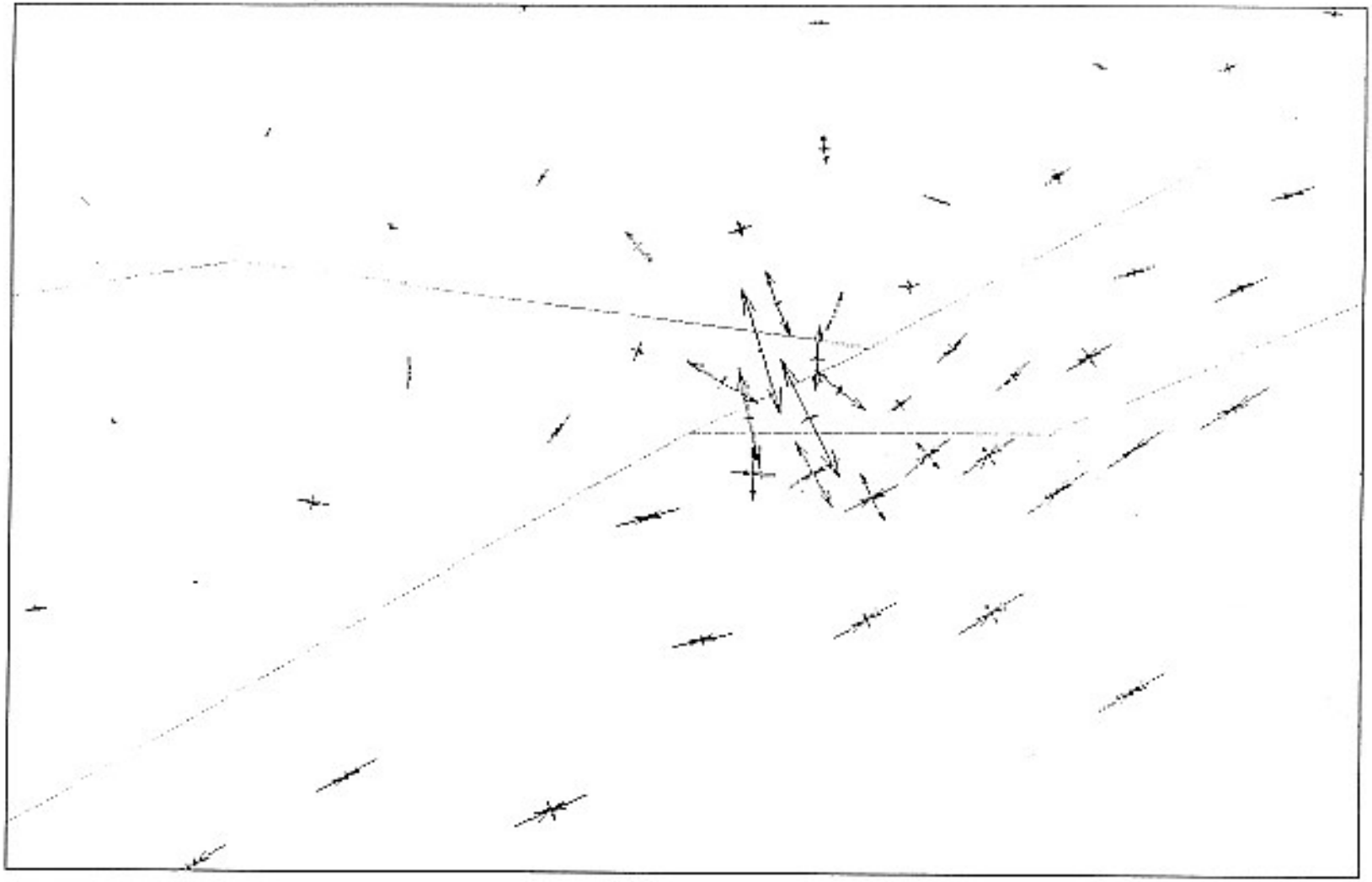

Fig.10c

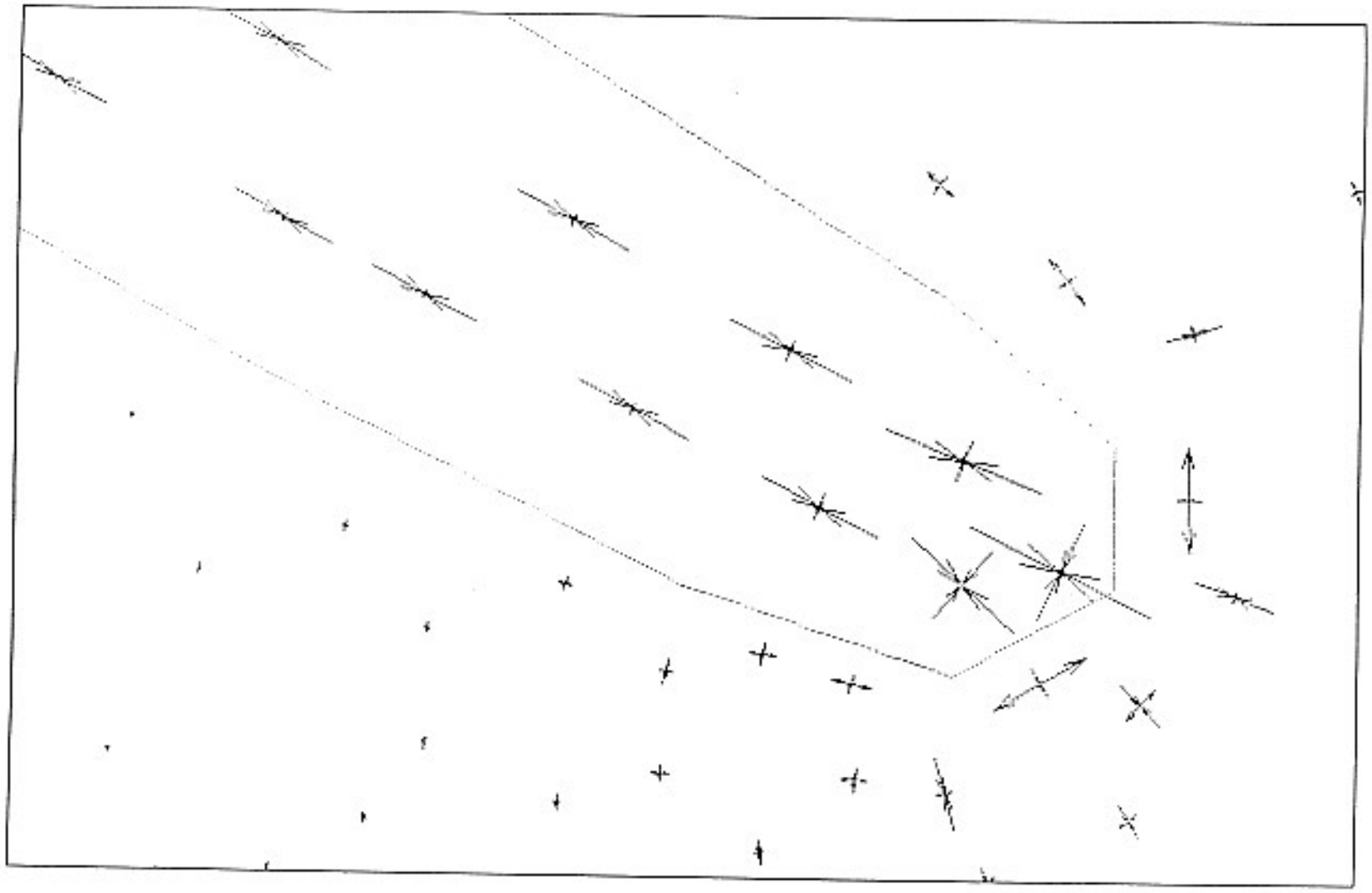

Fig.10d

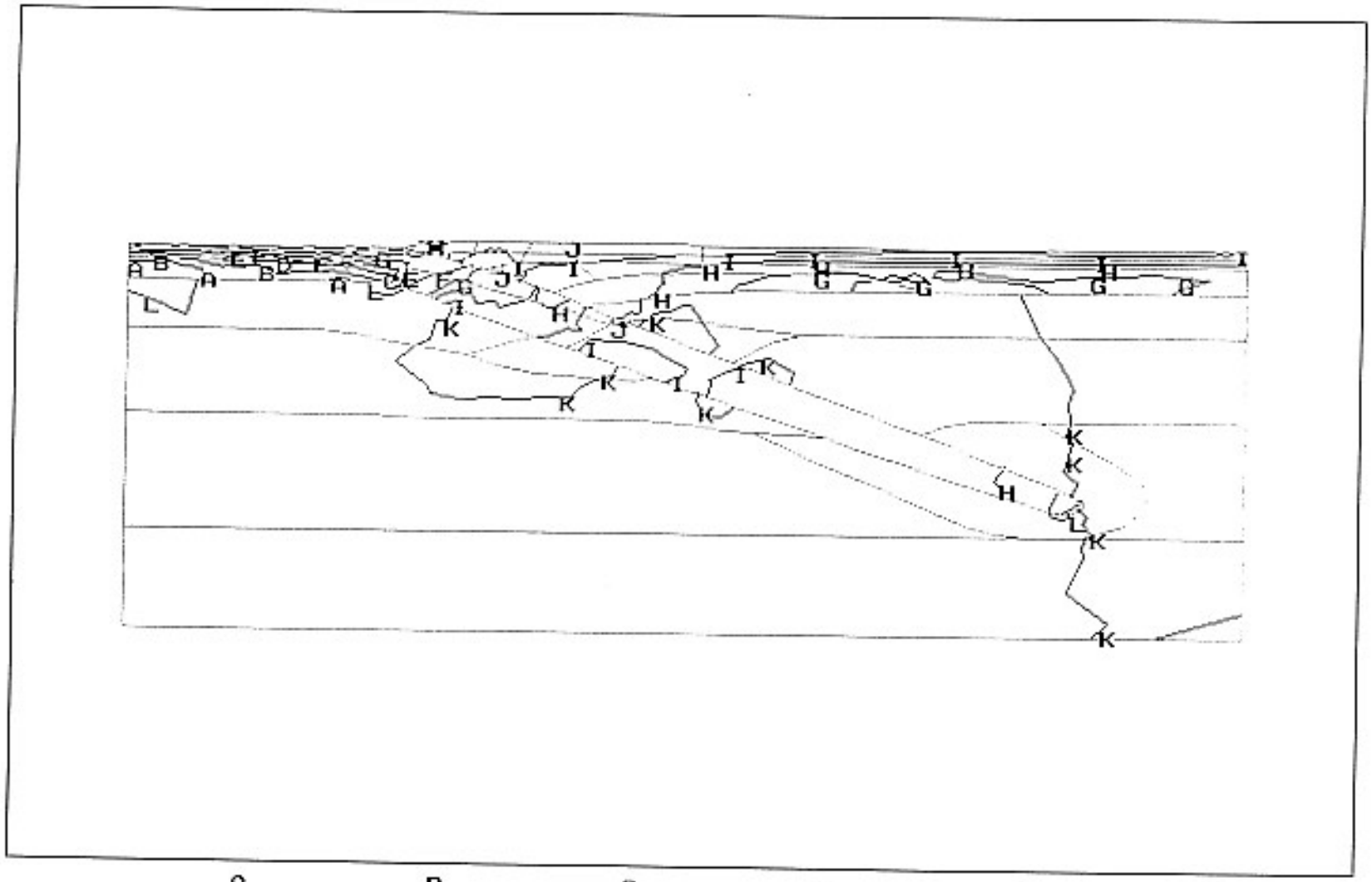

| | A | B | C | D | E | F |
|---|---|---|---|---|---|---|
| Sx | -2.524e+09 | -2.274e+09 | -2.024e+09 | -1.773e+09 | -1.523e+09 | -1.273e+09 |
| | G | H | I | J | K | L |
| | -1.023e+09 | -7.728e+08 | -5.225e+08 | -2.723e+08 | -2.203e+07 | 2.282e+08 |

Fig.10e

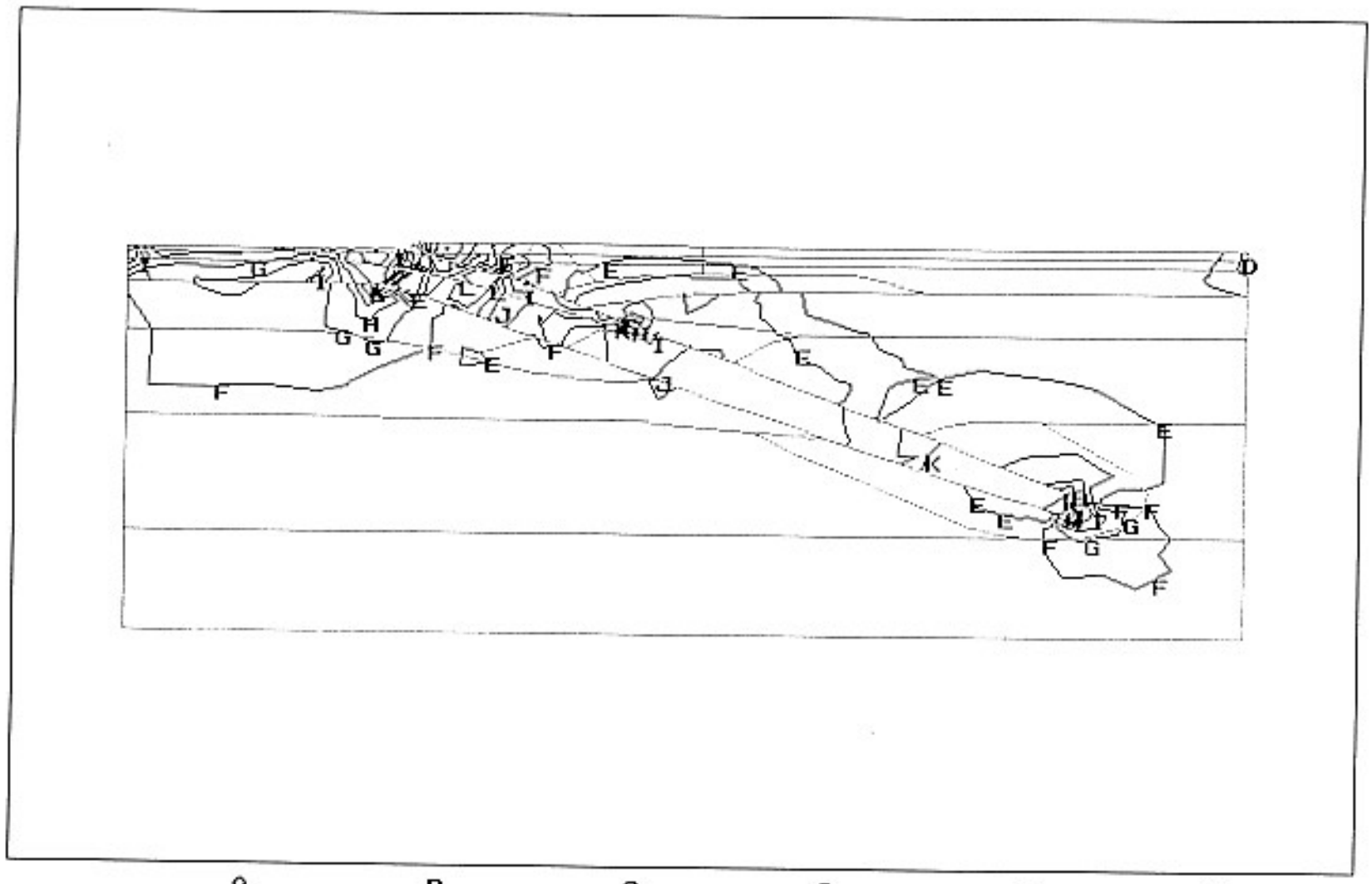

| | A | B | C | D | E | F |
|---|---|---|---|---|---|---|
| Sxz | -2.755e+08 | -2.129e+08 | -1.503e+08 | -8.767e+07 | -2.504e+07 | 3.758e+07 |
| | G | H | I | J | K | L |
| | 1.002e+08 | 1.628e+08 | 2.254e+08 | 2.881e+08 | 3.507e+08 | 4.133e+08 |

Fig.10f

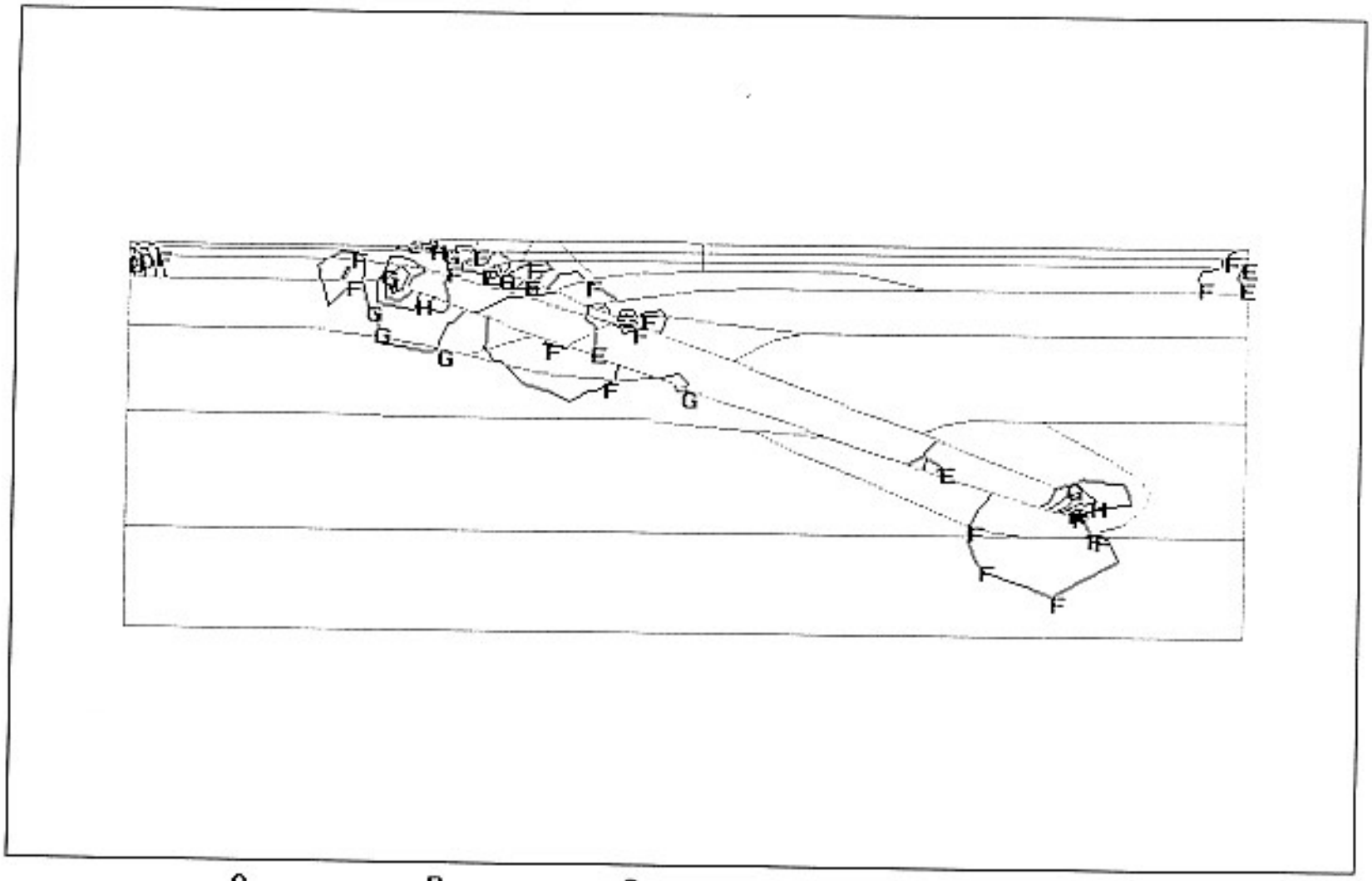

| | A | B | C | D | E | F |
|---|---|---|---|---|---|---|
| Sz | -8.852e+08 | -7.204e+08 | -5.556e+08 | -3.909e+08 | -2.261e+08 | -6.138e+07 |
| | G | H | I | J | K | L |
| | 1.033e+08 | 2.681e+08 | 4.329e+08 | 5.976e+08 | 7.624e+08 | 9.272e+08 |

Fig.10g

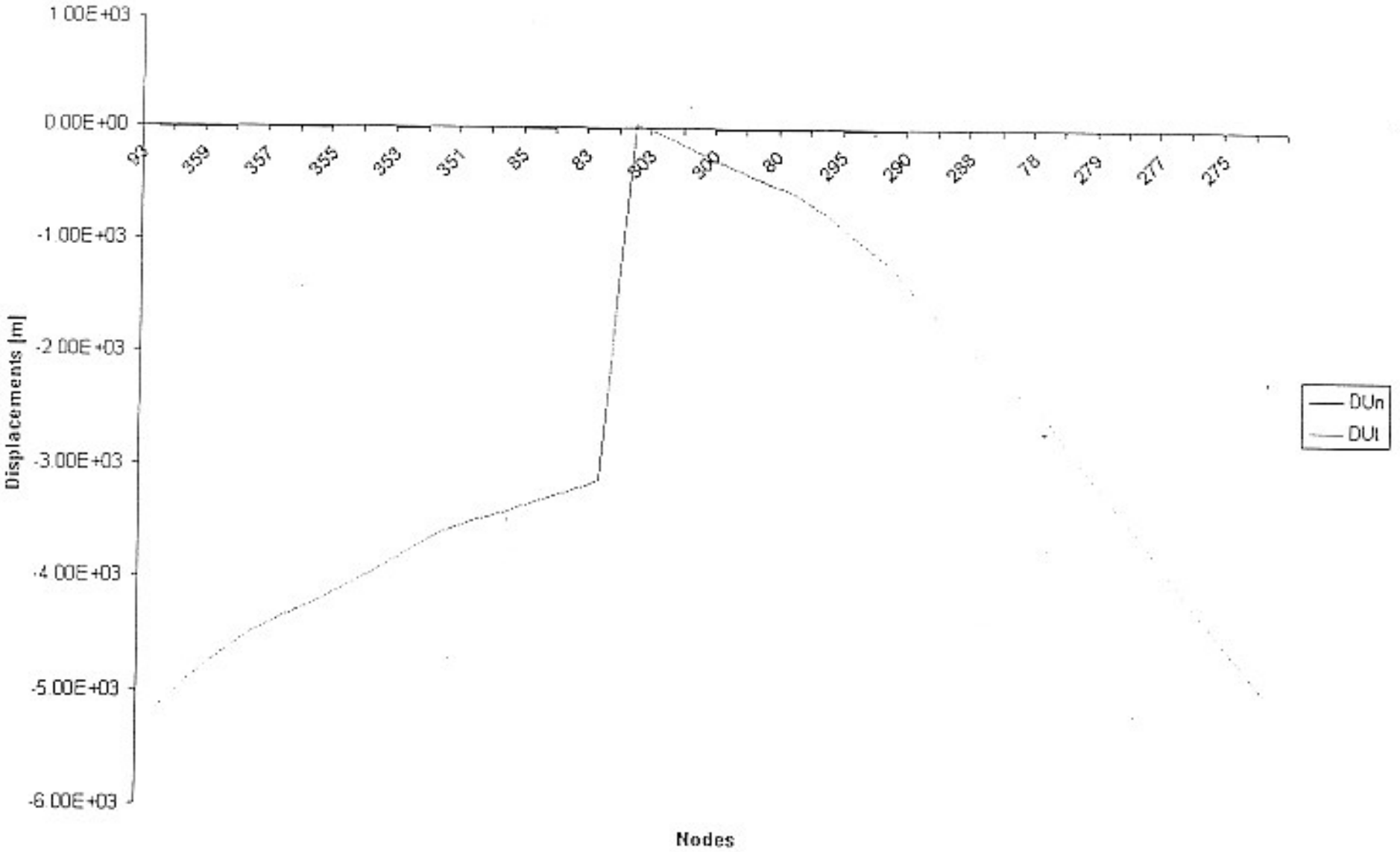
1.00E+03
0.00E+00
-1.00E+03
-2.00E+03
-3.00E+03
-4.00E+03
-5.00E+03
-6.00E+03
Displacements [m]
361
359
357
355
353
351
85
83
803
300
80
295
290
288
78
279
277
275
Nodes
DUn
DUt

Fig.11a

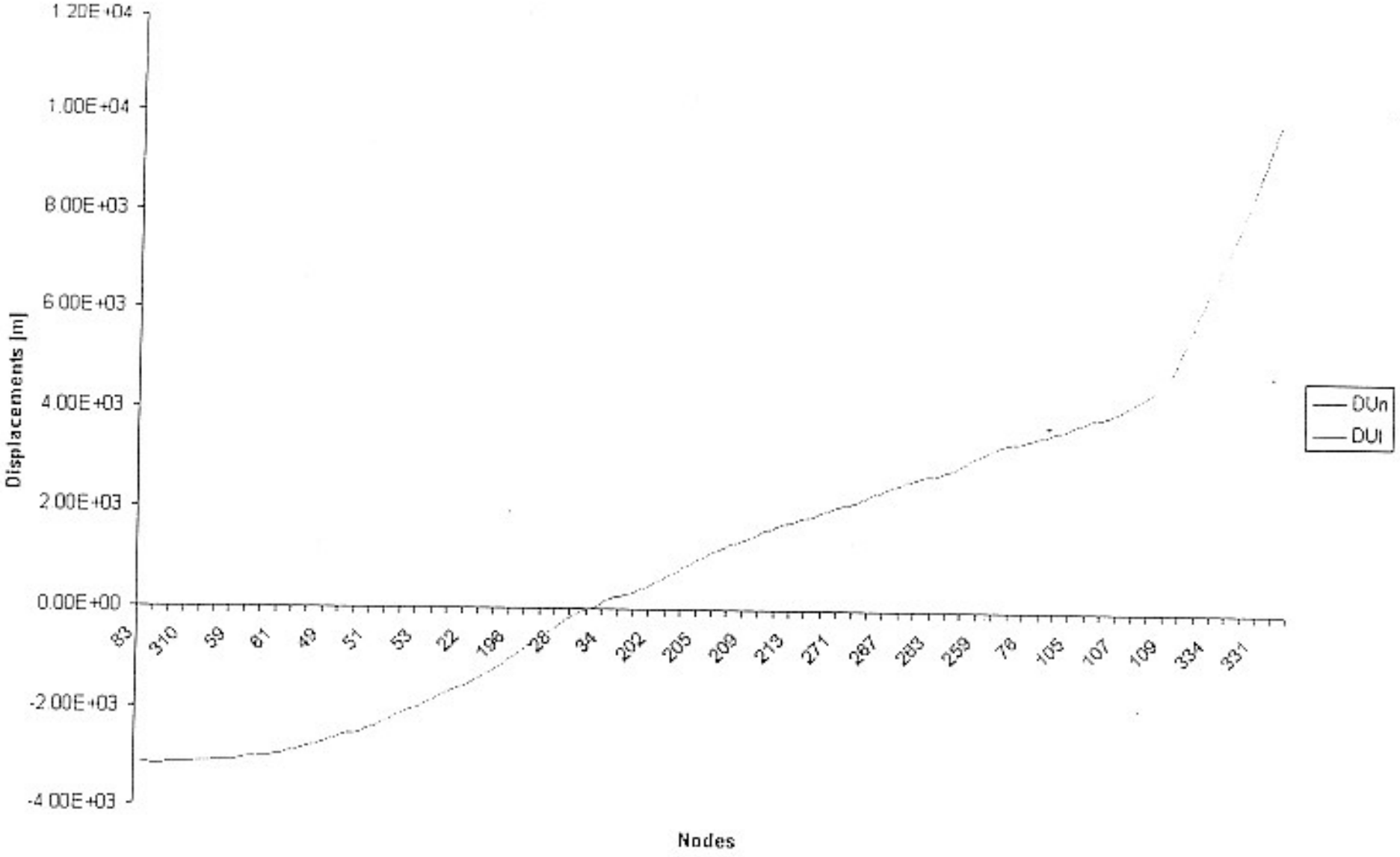
1.20E+04
1.00E+04
8.00E+03
6.00E+03
4.00E+03
2.00E+03
0.00E+00
-2.00E+03
-4.00E+03
Displacements [m]
83
310
59
61
49
51
53
22
198
28
34
202
205
209
213
271
287
283
259
78
105
107
109
334
331
Nodes
DUn
DUl

Fig.11b

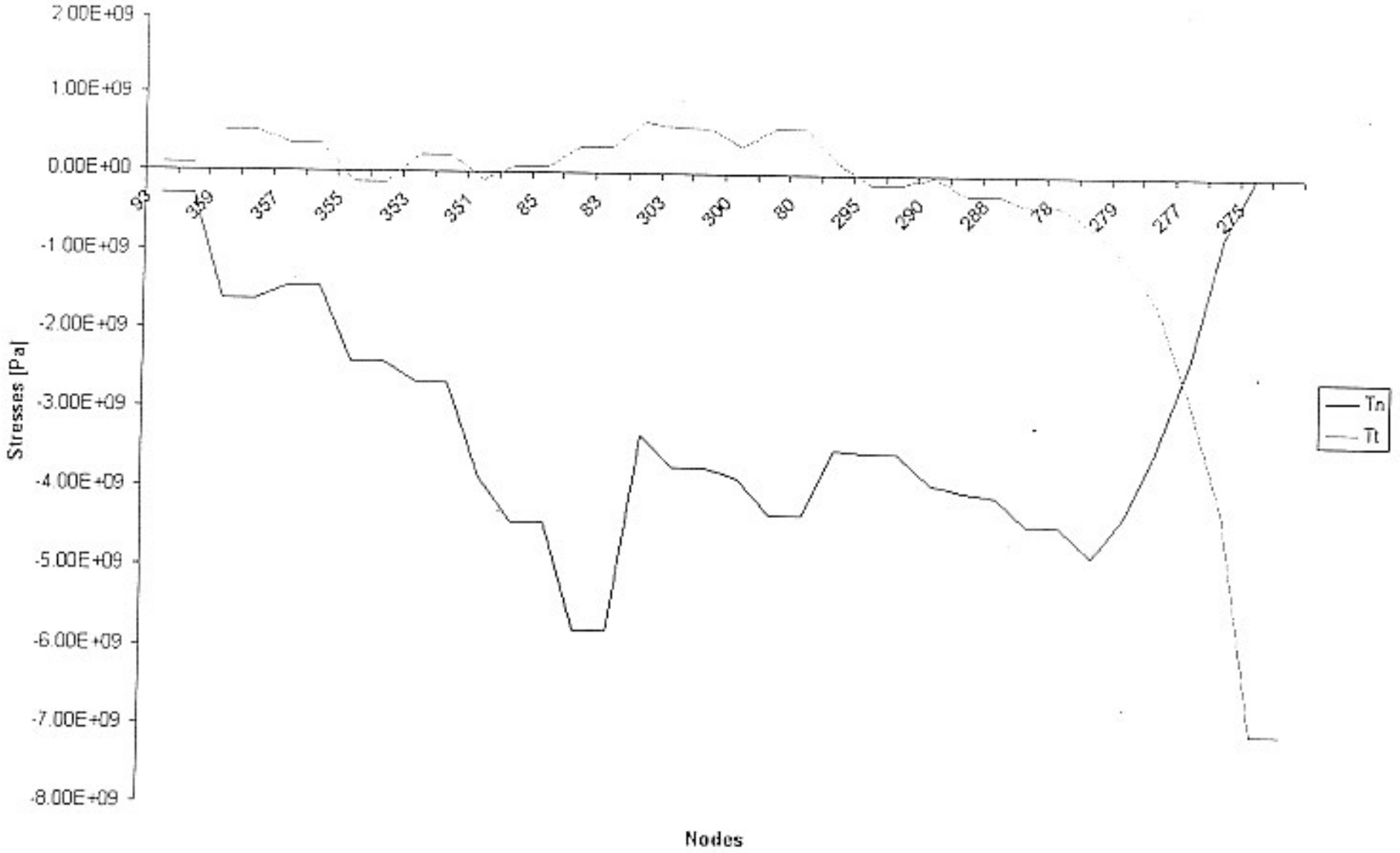
2.00E+09
1.00E+09
0.00E+00
-1.00E+09
-2.00E+09
-3.00E+09
-4.00E+09
-5.00E+09
-6.00E+09
-7.00E+09
-8.00E+09
Stresses [Pa]
93
359
357
355
353
351
85
83
303
300
80
295
290
288
78
279
277
275
Nodes
Tn
Tt

Fig.12a

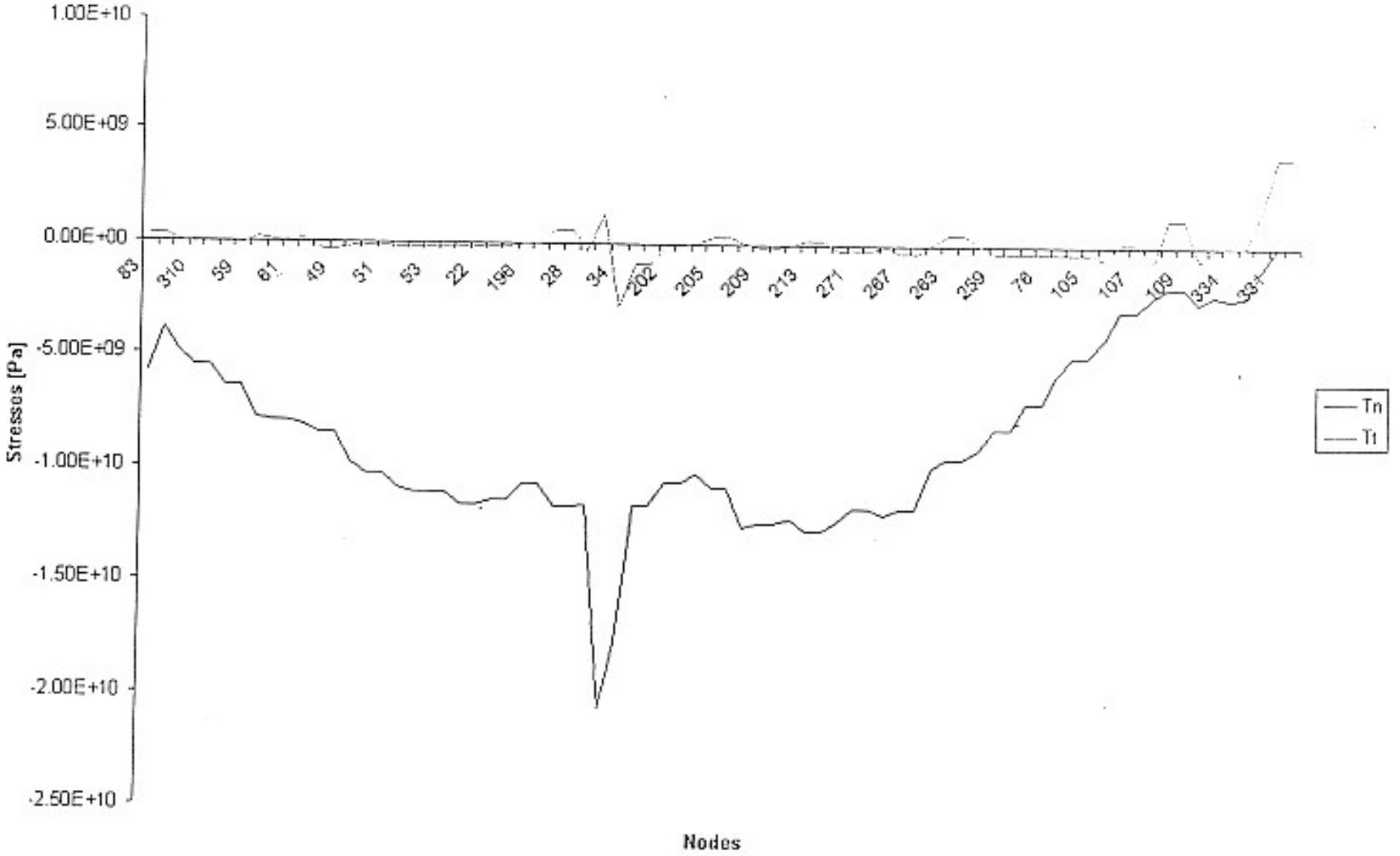
1.00E+10
5.00E+09
0.00E+00
-5.00E+09
-1.00E+10
-1.50E+10
-2.00E+10
-2.50E+10
Stresses [Pa]
83
310
59
61
49
51
53
22
198
28
34
202
205
209
213
271
267
263
259
78
105
107
109
334
33
Nodes
Tn
Tt

Fig.12b

List of figures



(†) Department of Geophysics and Astronomy, University of Sao Paulo, Brazil
*E-mail address*: berrocal@iag.usp.br

(‡) Institute of Computer Science AS CR, 182 07 Prague 8, Pod vodárenskou vezí 2, Czech Republic
*E-mail address*: nedoma@cs.cas.cz, nedoma@uivt.cas.cz